

The code **R_{x,y}** was applied to connect the comments of the reviewers with the changes done in the manuscript. **x** is the number of the reviewer and **y** is the number of the comment of the review **x** associated to a change in the manuscript.


Author's answers to Anonymous Referee #1

This is an important manuscript presenting data from repeat sections in the Southern Ocean south of Australia. The data analysis is comprehensive and the results are interesting and seem to be robust; they can be compared with other studies from the Southern Ocean, thus completing the view of this vital ocean region.

Thank you very much for your words.

Actually, I think there are even a few more studies that have recently appeared and addressing similar issues in other areas of the Southern Ocean, which the authors could incorporate in the discussion of the results.

We provide comparisons to many-recent works (12 studies published between 2007 and 2017, 9 of them since 2014). If the referee recommends comparison to specific works beyond these, we are open to consider it.

 The authors explain their results through the intensification of winds due to changes in the SAM. Their repeats cover the time period 1995 to 2011. However, they also write, almost at the beginning of the Discussion: "Several studies have reported a trend in the SAM toward its positive phase from the 1960s until the 2000s (Thompson and Solomon, 2002; Marshall, 2002, 2003; Lenton and Matear, 2007; Sallée et al., 2008)." During at least the second half of the time period, the SAM has not been in its positive phase anymore, and thus there will probably not be elevated winds anymore, which will not enhance upwelling. I encourage the authors to identify this and add comments to the manuscript.

The referee is correct. The SAM does not present a constant positive phase from 2000. However, it does exhibit considerable interannual variability, including, for the years 2008 and 2011 (two last occupations of SR03), relatively high SAM index values comparable to those at the end of the positive trend (<https://climatedataguide.ucar.edu/climate-data/marshall-southern-annular-mode-sam-index-station-based>), indicating strong winds over the region. This is shown in Figure A2, which will be added in the supplementary material:

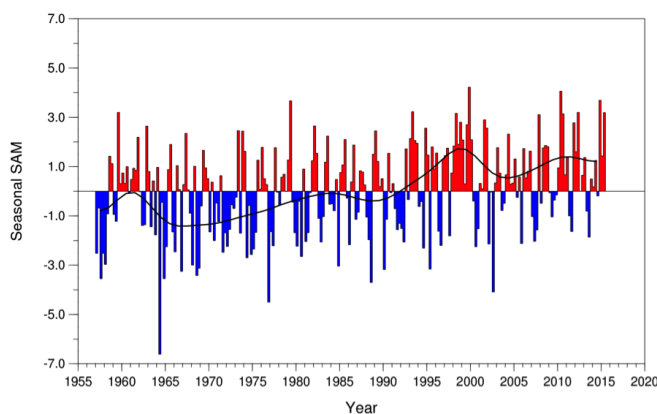


Fig. A2. Seasonal values of the observation-based SAM index. The smooth black curve shows decadal variations. Figure obtained from Marshall, Gareth & National Center for Atmospheric Research Staff (Eds). "The Climate

Data Guide: Marshall Southern Annular Mode (SAM) Index (Station-based)." Retrieved from <https://climatedataguide.ucar.edu/climate-data/marshall-southern-annular-mode-sam-index-station-based>.

Lines 27-29 of the Abstract will be corrected to:

"From all our results, we conclude a scenario of increased transport of deep waters into the section and enhanced upwelling at high latitudes for the period between 1995 and 2011 linked to strong westerly winds."

Line 23 in the Discussion section will be changed to:

" ... linked to strong westerly winds."

At the end of the first paragraph of the Discussion section we'll add:

"From the 2000s on, the SAM index no longer presents a positive trend but, although exhibiting considerable interannual variability (Fig. A2 in the supplementary material), the SAM index remains in its positive phase, favouring strong winds over the region."

R1.2) Although all cruises used for the analysis were conducted around summer, they were not in the same month. Actually, data may be 3-4 months apart. Certainly, in the deeper water masses, this will not have a big effect on the results. However, for the surface and sub-surface layers the seasonal changes in biologically-mediated properties are large and thus this is likely to have an effect on the computed rates. I think this caveat should be treated in the manuscript. Please comment on this and analyze the possible and expected effects on the results.

The effect of the seasonal variability is implicitly included in the errors of the trends and strongly reflected in the RMSE values within each water mass. That is why we only show statistically significant trends.

To clarify further, we'll change lines 14-15 of page 7 (section 3.3) to:

"We show the value of the root mean square error (RMSE or square root of the variance of the residuals), which can be interpreted in large part as unexplained variance caused by short-time scale processes including the different seasonal timings of the cruises. RMSE has the same units as the response variable."

R1.3) P1, line 11: Is this the correct symbol for neutral density (also at other places in the manuscript)?

No, it's not. Thanks for noticing. The epsilon will be changed to a gamma throughout the reviewed manuscript.

R1.4) P2, line 6 " : : : and ultimately upwell close to the Antarctic Shelf" I think this only holds for part of this water, and possibly not even the major part. Please change the wording to take that into account.

The referee is right. We'll modify the text in page 2 lines 5-6 to:

"...and ultimately upwell between the Southern ACC Front and the Polar Front."

R1.5) P2, line 11 I suggest a modified sentence: Within the eastward flow of the ACC major water exchange between the three ocean basins takes place.

Thanks. We accept this modification.

R1.6) P2, line 16 Because of twice the word “that” in this sentence I suggest: : : : water mass properties and this may complicate : : :

Thanks. We’ll correct this.

R1.7) P2, line 19 I think it is fair to cite older work of observationalists here, which actually laid the basis for this knowledge.

You are right. Two more references will be added:
“Sabine et al., 2004; Gruber et al., 2009”

R1.8) P3, line 12-13 Change to : : : reported an increase in CANT uptake : : :

Thanks. We’ll correct this.

R1.9) P3, line 16 delete “of the”

Thanks. We’ll correct this.

R1.10) P3, line 23 Change to : : : one of the most revisited sections in the Southern Ocean.

Thanks. We’ll correct this.

R1.11) P3, line 23-25 This sentence is an anacoluthon. Please correct.

Sorry for that. The sentence will recover the missing verb:

“Trends in oxygen (O_2), nutrients, and the carbon system parameters, i.e., DIC, total alkalinity (TA), anthropogenic carbon (C_{ANT}), total pH (pH_T) and % aragonite saturation (Ω_{Ar}) were estimated for the period 1995-2011, when both DIC and TA measurements are available.”

R1.12) P3, line 31 This concerns surface waters, I presume. Please add that term.

Yes, you are right. We’ll change line 31 in page 3 (section 2) to:

“separates warm, salty subtropical surface waters from cooler and fresher sub-Antarctic surface waters.”

R1.13) P4, line 30 Is there a reference for this?

Yes, it was included in the previous phrase. The reference (*Rintoul, 1998*) will be added in this phrase as well.

R1.14) P5, line 13-15 You only give the precision for DIC and TA measurements. Please also supply the accuracy, which is much more important here. It should be less good than the precision.

Thanks for noticing. We’ll change the phrase to:

“The precisions and accuracy of DIC and TA measurements improved slightly on more recent sections, and for all sections were better than $\pm 2 \mu\text{mol kg}^{-1}$, for both variables, based on analysis of duplicate samples and certified reference material”.

R1.15) P6, line 2 combined with and

Thanks. We'll correct this.

R1.16) P7, line 12 : : : defined by their $\text{I}\check{\text{S}}\text{n}$ condition (Table 2).

Thanks. We'll add this.

R1.17) P8, line 8-9 “Nevertheless, long-term trends in O_2 due to circulation and remineralization processes have not yet been reported.” This is not correct. See:

Matear, R. J., A. C. Hirst, and B. I. McNeil (2000), Changes in dissolved oxygen in the Southern Ocean with climate change, *Geochem. Geophys. Geosyst.*, 1, 1050, doi:10.1029/2000GC000086. (cited in the present manuscript)

van Heuven SMAC, Hoppema M, Jones EM, de Baar HJW, 2014. Rapid invasion of anthropogenic CO_2 into the deep circulation of the Weddell Gyre. *Phil. Trans. R. Soc. A* 372: 20130056. <http://dx.doi.org/10.1098/rsta.2013.0056>

We agree with the referee that this phrase is not correct and that our summary of previous work on this issue was not complete. The intention was to indicate that statistically significant trends *different from zero* in surface waters had not been reported, rather than that no investigations had occurred. With respect to the two studies mentioned, we accordingly note that neither found statistically significant trends in surface waters (except in the deepest layer of waters in the Weddell Sea in Van Heuven et al., 2014).

In order to clarify this, we'll change the text in 3.3 to (new text is underlined):

“The term $\frac{\partial \text{DIC}^{\text{BIO}}}{\partial t}$ can be influenced by changes with time of alkalinity due to changes in the rate of carbonate precipitation/dissolution and of AOU due to changes in the rate of remineralization and in circulation. In the present study only surface waters of the SR03 section present changes DIC^{BIO} between 1995 and 2011. Numerous studies have reported a strong influence of biological communities in the seasonal cycle of dissolved O_2 in surface waters (Bender et al., 1996; Moore and Abbott, 2000; Sambrotto and Mace, 2000; Trull et al., 2001a). Interannual variability in O_2 in upper layers of the Southern Ocean have also been related to changes in the entrainment of deeper waters into the mixed layer due to the mixed layer depth variability (Matear et al., 2000; Verdy et al., 2007; Sabine et al., 2008; Sallée et al., 2012). Although some studies found long-term decreases in O_2 due to circulation in deep waters of the Weddell Sea (van Heuven et al., 2014) and for the first 1000 m of the global ocean (Helm et al. 2011**), significant long-term trends in O_2 due to circulation and remineralization processes have not yet been reported for surface waters of the Southern Ocean.”*

*van Heuven, S., Hoppema, M., Jones, E.M., de Baar, H.J.W.: Rapid invasion of anthropogenic CO_2 into the deep circulation of the Weddell Gyre. *Phil. Trans. R. Soc. A* 372: 20130056. <http://dx.doi.org/10.1098/rsta.2013.0056>, 2014.

** Helm, K. P., Bindoff, N.L., and Church, J.A.: Observed decreases in oxygen content of the global ocean, *Geophys. Res. Lett.*, 38, L23602, doi:10.1029/2011GL049513, 2011.

We'll also add some comments in section 5, (after first paragraph in page 13) in order to acknowledge previous efforts:

"In terms of the change in oxygen, Helm et al. (2011) found an average decrease in the concentration of O_2 between 100 and 1000 m from 1970 to 1992 of $\sim -0.23 \mu\text{mol l}^{-1}$ for the Southern Ocean (27% of the estimated global average change, $-0.93 \pm 0.23 \mu\text{mol l}^{-1}$). Considering the volume of the first 1000 m of the water column of the Southern Ocean to be $19400 \cdot 10^9 \text{ l}$ (obtained using ETOPO1 doi:10.7289/V5C8276M) and the volume of the first 1000 m of the SR03 section to be $2700 \cdot 10^9 \text{ l}$, the decrease of O_2 found by Helm et al. (2011), if constant in time, would correspond to a decrease of $\sim -1.7 \mu\text{mol l}^{-1} \text{ yr}^{-1}$. We only found changes in oxygen within the surface water mass layers (STCW, AASW and AASW_{upw}) that approximately fill the first 300 m of the water column of the SR03. Then, the decrease of $\sim -1.7 \mu\text{mol l}^{-1}$ would correspond to an average change of O_2 of $\sim -0.32 \mu\text{mol kg}^{-1} \text{ yr}^{-1}$ for surface waters of the SR03. This means that values of $\sim 0.20 \mu\text{mol kg}^{-1} \text{ yr}^{-1}$ due to circulation processes can be expected in $\frac{\partial \text{DIC}^{\text{BIO}}}{\partial t}$ for surface waters, which is comparable to the average of our findings (Table 5), $0.32 \pm 0.24 \mu\text{mol kg}^{-1} \text{ yr}^{-1}$ and could indicate that the change in O_2 is related to circulation processes."

R1.18) The last paragraph of section 5 is clearly a conclusion, and should thus be moved to the Conclusions section.

We agree. Thanks. We will move this paragraph.

R1.19) P15, line 13 delete one "repeat"

Thanks. We'll correct this.

R1.20) P16, line 8 uses stepwise MLR (delete "and")

Thanks. We'll correct this.

R1.21) P18, lines 16-17 This sentence is incomplete.

We'll complete the sentence:

"A battery of OMP analyses were done with varying values of R_N between 9 and 10 in increments of 0.2, R_P between 120 and 145 in increments of 5, and R_{Si} between 0 and 8 in increments of 2."

R1.22) P23, line 8 When using data from GLODAPv2, please cite GLODAPv2 manuscript, Olsen et al 2016 ESSD.

The references will be added:

Key et al., 2015; Olsen et al., 2016 in section 3.1

Lauvset et al., 2016 in section A.3 page 23

R1.23) P24, line 31 delete info near end of line

Thanks. We'll correct this.

R1.24) P25, line 24 Deep-Sea (hyphen)

Thanks. We'll correct this.

R1.25) P27, line 6 Deep-Sea (hyphen)

Thanks. We'll correct this.

R1.26) P27, line 22 add NCAR technical note

Thanks. We'll correct this.

R1.27) P27, line 26 Law et al. as shown here is the Discussions paper. There is also a final paper in Geosci. Model Dev. from 2017.

The reference will be changed to Law et al. (2017):

“Law, R. M. et al.: The carbon cycle in the Australian Community Climate and Earth System Simulator (ACCESS-ESM1) Part 1: Model description and pre-industrial simulation, Geosci. Model Dev., 10, 2567–2590, <https://doi.org/10.5194/gmd-10-2567-2017>, 2017.”

R1.28) P32, line 11 Comptes Rendus Geoscience

Thanks. We'll correct this.

R1.29) P32, line 26 Mechanisms (typo)

Thanks. We'll correct this.

R1.30) Table 2 caption: references (typo)

Thanks. We'll correct this.

R1.31) PF is defined in the caption but does not occur in Table 2

Thanks. We'll correct this.

Author's answers to Referee #2 (Dr. Marta Álvarez)

This manuscript (MS) is a very nice piece of work dealing with real biogeochemical data in the Southern Ocean south of Tasmania. As an biogeochemical observationist I do really appreciate high quality sustained ocean observations in harsh regions as the SO. Maintaining the funding for such expensive long term programs is always difficult. State agencies always prefer quick, 3-4 years projects with high impact results for society or policy makers. The slow science done with time series, either fixed or oceanographic lines is precious to detect global change in a comprehensive way (Henson, 2014, [dx.doi.org/10.1098/rsta.2013.0334](https://doi.org/10.1098/rsta.2013.0334)).

Thank you very much for your comment. We really appreciate it and the very thorough review, which has added to the paper.

After the nice words, I do conclude that this MS should be accepted but before, it needs some MINOR improvements, they regard to two main points organization and data & calculations.

With regard to the organization of the MS:

- the resolution or uncertainty of the back-calculation method for CANT is given in page 16, line 16. It should be given in section 3.2.

The uncertainty of C_{ANT_BC} was already mentioned in section 3.2 (page 6, line 4).

- I would suggest including section 6 as Supplementary material, a slight change in the organization / order of this section, the general title is OK for me, but the sections would be:

Thank you very much for the advice. Nevertheless, we consider that section 6 should stay as it is for two main reasons:

- When talking about C_{ANT} it is always good to have some reference values from other methodologies.
- Explaining the sensitivity of the results completes the manuscript and explores the reliability of the results.

Besides, the scheme proposed for the inclusion of section 6 in the supplementary material does not change too much the structure of section 6 as it is right now.

The numerical model configuration, the OMP analysis and the particularities of the AT0 and CDIS estimates should be in the supplementary material to make the reading in the main text easier. In fact, we think that it could be better to upload this supplementary material in a separate file.

Before continuing, there are some points that we would like to clarify. There has been a misunderstanding with the methodology, mainly because we misled the sign in equation 3 and also because we need to clarify certain aspects of the methodology. Also, we think that there was a misunderstanding between this work and the previous work by Pardo et al. (2014), probably favoured by the error in the sign of Equation 3. We would like to clarify that we refer to Pardo et al. (2014) because the methodologies are similar. Since a similar methodology was applied before in the Southern Ocean we consider that it is fair to cite this reference. Nevertheless, we do not redirect the reader to that

work because we prefer to explain the methodology again in order to help readers not familiar with back-calculation methods. We will try to clarify this in the following answers.

We answered the comments as they were made, i.e., following the proposed organization. We did not answer those comments that are just a title for the proposed organization scheme.

- CANT estimation

If this comment refers to moving section 3.2 to the supplementary material, we do not agree. We would like to maintain the methodology in the main text in order to help readers not familiarized with back-calculation methods.

- OMP analysis

- parameterization for TA0 and CDIS - biogeochemical model estimating $\delta CDIS$, please give numbers for this term, as far as I understand is not given in Table A1.

$\delta CDIS$ can be easily obtained through Eq. 4 (section 3.2):

$$CDIS^{\pi} = CDIS - \delta CDIS$$

and for this reason we do not list it separately (redundantly) in Table A1.

- DIC changes

- CANT estimated with other methods

R2.1) - circulation and biological processes at steady state: here I have doubts & thoughts, the methodology to calculate DIC changes and attribute them to any oceanographic process (C_{ANT} increase, change in circulation, warming, higher upwelling,..) should be clarified in the main MS.

We agree with Dr. Álvarez in that there is a need to clarify more the estimates of the change in DIC explained in section 3.3. We will add the next text after the first paragraph of section 3.3:

“Respect to the total change of DIC ($\frac{\partial DIC}{\partial t}$), our goal is to disentangle the effects that solubility, circulation, biology and C_{ANT} uptake have on the variability of DIC. The total change of DIC ($\frac{\partial DIC}{\partial t}$) in a water mass is due to changes in the atmosphere-ocean exchange, biological processes and circulation processes. In order to account for the change in DIC due the atmosphere-ocean exchange and biological processes, we compare $\frac{\partial DIC}{\partial t}$ to $\frac{\partial C_{ANT-BC}}{\partial t}$ and $\frac{\partial DIC^{BIO}}{\partial t}$, Eq. (2). The change in DIC not explained by $\frac{\partial C_{ANT-BC}}{\partial t}$ or $\frac{\partial DIC^{BIO}}{\partial t}$ will then be due to circulation processes.

In order to compare $\frac{\partial DIC}{\partial t}$ to $\frac{\partial C_{ANT-BC}}{\partial t}$ we need to consider how the change in $\frac{\partial DIC^{BIO}}{\partial t}$ and DIC^{π} ($\frac{\partial DIC^{\pi}}{\partial t}$) (terms of Eq (1), section 3.2) affect the changes in C_{ANT-BC} .”

We believe that all the following comments also belong to this same point: “- circulation and biological processes at steady state”. We will answer them individually following the assigned numbers.

R2.2):

- 1) On one side, the BC method for CANT assumes steady state in the circulation / biology (= constant stoichiometric ratios), the main reason behind is that biology activity or ocean circulation/mixing is not affected by the CANT increase.
- 2) On the other side, when talking about DIC is completely untrue that is not affected by changes in circulation (higher/lower upwelling, higher/lower transport of water masses).
- 3) Any change on circulation would be detected in AOU (as nutrients are always more problematic due to precision and exactitude issues).
- 4) But also in transient tracers that you do not show (this is an important caveat of the whole analysis!!).
- 5) Please clarify in this section which processes affect CANT and which DIC and how your method deals with them.

- 1) We agree and we stated that the C_{ANT_BC} assumes steady state in the circulation /biology (section 3.2):

“Back-calculation methods assume the ocean is in steady state for dynamical and biological processes.”

- 2) We agree. We never stated that the DIC is not affected by the changes in circulation. In section 3.3 we say:

“We assume that the changes in DIC^{BIO} due to circulation do not affect the amount of DIC in the layer. This assumption is one of the caveats of the methodology, since we cannot know how much of the change in DIC is associated to changes in circulation, i.e., how much of the change in DIC is a change in non-anthropogenic DIC. We will discuss this more in section 4.4.2.”

This comment made us realize that there is an error in the citing of section 4.4.2, which should be “section 6.2”. We’ll correct this.

We hope that the new text clarifying which processes drive the changes in DIC (please, see answer to the point: “- circulation and biological processes at steady state”) will help with this misunderstanding.

- 3) We agree and had already explained this aspect of AOU (section 3.3, page 8 lines 10-11):
“...since part of the changes in AOU with time reflect changes in circulation that we cannot separate from those in remineralization.”

We also agree with the comments on nutrients and, as well as the problematic precision of nutrients, we had already noted that upper ocean processes also impact their utility for trend detection:

“The detection of long-term trends of nutrients at upper layers of the ocean can be masked by short time scale physical processes such as changes in the mixed layer depth, mesoscale activity and advection.” (Section 6.2, page 16, line 32 and line 1 of page 17).

- 4) Unfortunately, using transient tracers is beyond the scope of this manuscript for several reasons:

- There are only CFCs available for all the cruises considered. Other tracers have been measured but not in all the cruises. CFCs alone are not the most reliable tracers when establishing water mass ages in young surface waters, places of frequently deep convection or in bottom waters that are eventually ventilated, because of their decay in the atmosphere.

- Most importantly, our main goal in the study is to make use of most data from the SR03 and also to consider the input of AABW in terms of C_{ANT} .

- 5) We will add a new text after the first paragraph of section 3.3 for further clarification. See answer to the comment on point: “- circulation and biological processes at steady state”.

R2.3) - changes in the rates of export of POC: POC export is related to primary production in the upper layer, higher POC production implies higher primary production. If this POC is mineralized AOU would increase and DIC increase as well, only if we keep the same circulation. An intensification of circulation for the same POC input would mean a lower AOU as bacteria would have less time to work. I insist that without transient tracers disentangling the influence on DIC from circulation and biology is difficult.

We agree that this disentanglement is challenging, and accordingly in section 6.3 we stated that:

“Our results show that the increase of DIC in mode and intermediate waters is fully explained by the uptake of atmospheric CO₂, which could indicate that there was no detectable change in the rate of export of POC over the 1995-2011 period.”

Moreover, we considered the change in the rate of export of POC as a possible reason for the increase of DIC in deep waters. That is why we considered the results from deep sediment traps:

“Estimates of POC export in the SAZ (~3800 m), the SAF (~3100 m) and the PFZ (~1500 m) using moored sediment traps..” to check how important a change in the rate of POC export could be on the DIC change found for deep water masses.

Nevertheless, we agree with the comment and we will clarify this further by changing the text at the end of the second paragraph of section 6.3 into:

“This increase is close to the uncertainty of the total DIC increase estimated for the UCDW layer, which means that in order to generate an increase in DIC similar to that found in the UCDW layer, the rate of POC export should be ~10 times higher than the observed rates. This change should be certainly noticeable in $\frac{\partial DIC^{BIO}}{\partial t}$ in surface waters but most probably in deep waters as well, which we do not see”.

- stoichiometric ratios

- the title of the MS is "carbon uptake and biogeochemical change", so I understand is not only CANT changes, it is mainly about DIC changes and the processes causing them, of course, one of them the CANT increase.

I do follow section 3.2, but I do not follow section 3.3. In fact I think section 3.3 should be introduced in first order compared to section 3.2.

This is part of the misunderstanding we were talking about before. We believe that section 3.2 is necessary to understand section 3.3, and therefore prefer not to reorder the text. We hope that with the explanations given it is clearer now.

R2.4) And I question in the current section 3.3 the explanations in page 8 to estimate CANT /DIC changes and the reasoning behind. It seems that two types of CANT are in the ocean, the back calculated and another one with something else. IT seems as well that CANT changes could also contain DIC changes related to AOU (circulation/biology) which is clearly separated in section 6. As section 3.3 is difficult to follow the results in Tables 4 & 5 too. I will comment more about this issue in the data & calculation section of this review.


There are not two types of C_{ANT} . C_{ANT_BC} is directly estimated using the back calculation method and $\frac{\partial C_{ANT}}{\partial t}$ is obtained by correcting $\frac{\partial C_{ANT_BC}}{\partial t}$ for the effects of solubility and change in DIC^{BIO} . $\frac{\partial C_{ANT}}{\partial t}$ is the best approximation for the change in C_{ANT} (as we already stated in section 3.3):

“We consider the best approximation for the change in C_{ANT} as a range depending on the possible effect of biology and circulation processes on $\frac{\partial DIC^{BIO}}{\partial t}$. If the value of $\frac{\partial DIC^{BIO}}{\partial t}$ is due to the variability in the remineralization rates and the change in solubility is considered, the estimate $\frac{\partial C_{ANT_BC}}{\partial t}$ will be the lower limit of the range, (lower limit of $\frac{\partial C_{ANT}}{\partial t} = \frac{\partial C_{ANT_BC}}{\partial t} + \frac{\partial DIC^\pi}{\partial t}$). For the upper limit of the range, we consider that the value of $\frac{\partial DIC^{BIO}}{\partial t}$ is due to changes in circulation and the upper limit of the range is obtained by $\frac{\partial C_{ANT}}{\partial t} = \frac{\partial C_{ANT_BC}}{\partial t} + \frac{\partial DIC^\pi}{\partial t} + \frac{\partial DIC^{BIO}}{\partial t}$.”

And we also repeated this during the explanation of the results (section 4.1.1) in order to help the reader.

We will add a new figure to improve the understanding of this differences between $\frac{\partial C_{ANT_BC}}{\partial t}$ and $\frac{\partial C_{ANT}}{\partial t}$:

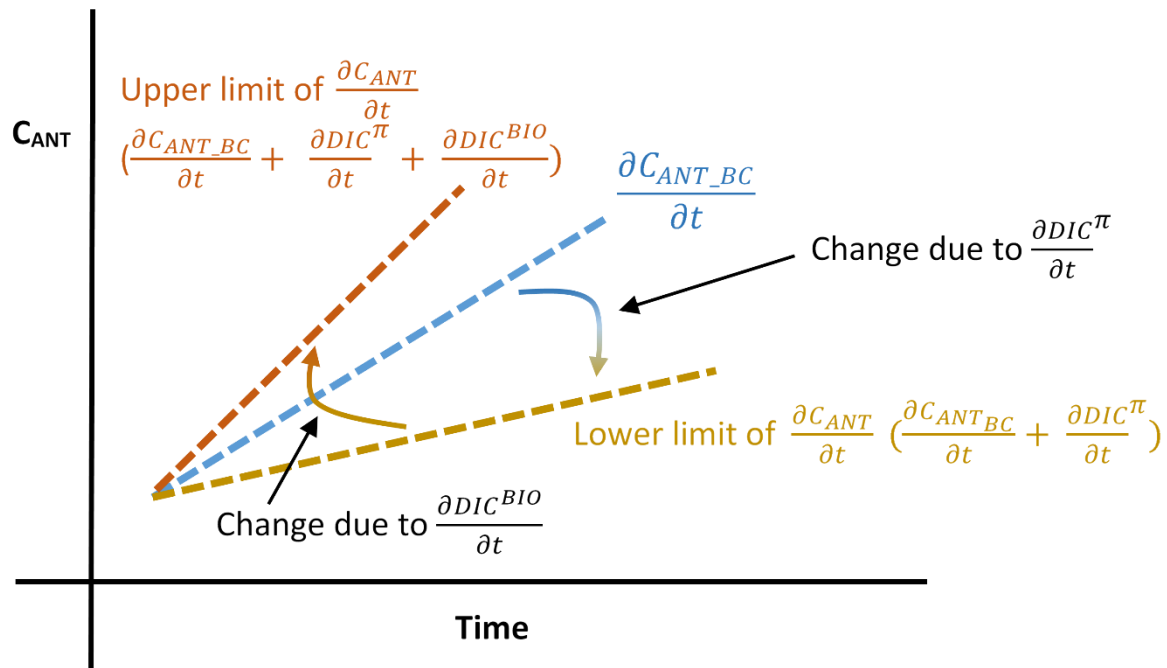


 **Figure:** Estimation of the ranges in $\frac{\partial C_{ANT}}{\partial t}$ from $\frac{\partial C_{ANT_BC}}{\partial t}$, depending on the possible effect of biology and circulation processes on $\frac{\partial DIC^{BIO}}{\partial t}$ (section 3.3).

- I do miss some figure with the temporal evolution of DIC & CANT & DICBIO at the different layers.

The temporal evolution is presented in Table 4 with the errors and RMSE. The trends in the table offer the same useful information that the figures of the temporal evolution.

- Table 6 should be included in the corresponding section of the Sup information if changes!

We've decided not to change the structure of the manuscript.

With regard to the data & calculations:

R2.5) - Cruise data: please state that those cruises were included in GLODAPv2 and therefore checked, DIC for the 2008 was corrected. Please confirm that there is no transient tracer data (CFCs or/and SF6).

We stated that the data are included in GLODAPv2 (page 5, lines 17-18) but we did not clarify the QC done to the variables. We'll change the phrase to:

“The section data are available through the Global Ocean Data Analysis Project (<http://cdiac.ornl.gov/oceans/GLODAPv2>; Key et al., 2015; Olsen et al., 2016). The original data for the different cruises were corrected following the QC recommendations in GLODAPv2.”

We already answered the comment about tracers.

R2.6) It is very very surprising to report oxygen accuracy and precision as 1%, please correct me if I am wrong, so for O₂ in deep bottom water, 230 umol/kg.. the estimation error would be 2.3 umol/kg, it means an error in DIC_{BIO} of 1.6 umol/kg. Quite high.

We agree. It was an error. The accuracy and precision for O₂ are 0.3% .

R2.7) - CO₂SYST calculation: please state that you calculate pHT and omega Ar in situ from DIC and TA. Which is the borate constant?.

We will make that clearer by changing the previous phrase (line 19 page 5):

“DIC and TA measurements allow estimates of other variables of the dissolved CO₂ system.”

To:

“Other variables of the dissolved CO₂ system were calculated from the DIC and TA measurements.”

And also the second sentence in the paragraph to:

“We calculate pH_T and Ω_{Ar} (from measured DIC and TA) using the CO₂sys program ...”

The reference for the borate constant is: Upström. (1974). It will be added in the text.

R2.8) - Table 3: which is the meaning of "*" for the 2011 cruise in the SAF region?

The explanation will be added to Table 3 caption:

“ The range in the location of the SAF for the 2011-cruise could be related to a diversification of the PF or SAF into different jets (Sokolov and Rintoul, 2009) but also to crossing the meander of the front twice.”*

- CANT estimation: either you include here current section 6.1 or you keep the CANT-OMP method as the only one, and the others in the Supl. Material

In order to understand the results we need to maintain the two different notations. $\frac{\partial C_{ANT}}{\partial t}$ is the best approximation we can offer to compare to $\frac{\partial DIC}{\partial t}$. We already explained the differences between $\frac{\partial C_{ANT}}{\partial t}$ and C_{ANT_BC} (or CANT-OMP, as you call it). We hope that adding the new Figure will help to understand this better.

With regard to the CANT-OMP method, the reference paper is Pardo et al. (2014), I suggest to use the same notation.

This is another misunderstanding. We would like to say that we use Pardo et al. (2014) as reference because the methodologies are similar but we never redirect the reader to that work. We already explained that we rewrote the methodology in order to help those readers not familiar with back-calculation methods.

Similarly to what we did before, we are going to answer the following comments using the assigned numbers.

R2.9):

- 1) Your Eq 1 defining CANT-OMP is different from Eq 4 in Pardo2014.
- 2) I always understood CANT as the difference in preformed conditions from now (or whenever) to preindustrial times. So what is the meaning of DIC^π in current Eq1, it should be DIC_0^π .
- 3) Current Eq 3 is also different from Eq 3 in Pardo2014.
- 4) The MS DIC^π is different from DIC_0^π ?? However current Eq 4 equals Eq4 in Pardo2014.
- 5) Table 1 in Pardo2014 and Table A1 & A3 here should be comparable.
- 6) Maybe in Table 1 2014 there is a typo ΔC_{dis}^π should just be ΔC_{dis} . I am very confused about the CANTOMP calculation for the disequilibrium term and the info given in Table 1 here and that in Pardo2014. Please clarify
- 7) And please give in the section the error for CANT-OMP.

- 1) Equation 4 in Pardo et al. (2014) is not the definition of C_{ANT_BC} (or CANT-OMP as you call it). Probably you refer to Eq. 1 in the present manuscript compared to Eq. 1 in Pardo et al. (2014). These equations are not exactly the same. Nevertheless, if you follow both texts a little, it is easy to find the similarity.
- 2) You understood correctly, CANT is the difference from preformed conditions. DIC^π is always a preformed variable. The notation in Pardo et al. (2014) relates to that used by Chen (1982)*. The “origin” of CANT for a water mass is: at preindustrial times and in its region of formation, which is the surface ocean. This means that DIC^π is always going to be a preformed value whatever the notation chosen. There is a small problem with the notation “0” in DIC^π . While Chen (1982) does not consider the disequilibrium term we do, thus the real “preformed” term should be DIC^π_{SAT} . That is why we decided to avoid the notation “0” this time. Nevertheless, to avoid more confusion, we will add “preformed” in the text when explaining the term DIC^π : a) in page 6 line 17: “...and DIC^π is the preformed concentration of DIC in preindustrial times.” and b) in page 6 line 28: “The preformed preindustrial term, DIC^π , ...”.

*Chen, C.-T. A.: On the distribution of anthropogenic CO_2 in the Atlantic and Southern Ocean, Deep-Sea Research, 29, 5, 563-580, 1982.

- 3) Thank you very much for noticing. We made a mistake with the sign of Eq. 3 and it will be corrected.

$$DIC^\pi = DIC^\pi_{SAT} + CDIS^\pi$$

It was just a typo in the equation, the estimates were done correctly.

4) Yes, those equations are and should be the same. All is okay.

5) The tables are not equal but are comparable.

In Pardo et al. (2014) Table 1 is shorter than Table A1 (present manuscript) because there was a previous manuscript describing the OMP analysis (Pardo et al., 2012) done for the whole Southern Ocean, which was the base for the study of CANT in Pardo et al. (2014). Nevertheless, we'll add the uncertainties of the parameters of definition of the SWTs to Table A1 in order to make them more comparable

In the present manuscript, we changed some things in the OMP analysis with respect to Pardo et al., (2012) because this is a local study. In a local study it is really important to consider the local varieties of the water masses in order to maintain the reliability of the OMP. This is why we have to show the whole definition of the SWTs in Table A1.

With respect to Table A3 (present manuscript) comparison to Table 1 in Pardo et al. (2014), we consider that this is just a matter of how you present the equations. In detail, the way we estimated AT^0 and CDIS in the current manuscript is similar but not identical to how it was done in Pardo et al. (2014).

6) There is no typo in Table 1 of Pardo et al. (2014) and ΔC_{dis} can be estimated with the equation 4 given in Pardo et al. (2014).

7) The error for C_{ANT_BC} is already given there (page 6, line 4).

The reference for Thacker 2012 is not included in the references.

The reference is already in the previous manuscript.

R2.10) Silicate is included as a non-conservative variable in the OMP, but no Ratio is given.

Silicate is included as a conservative variable and no Ratio is needed. We mentioned that in section 6.4: *"The residuals of SiO₄ did not change significantly for any value of R_{Si} and we consider SiO₄ as a conservative variable."*

But we forgot to mention it in section A.2 where it should be. Thanks for noticing. We would add this information in section A.2.

R2.11) I think is more coherent to write ΔO_2 in the section A.2.

We agree. We'll change ΔO to ΔO_2 .

R2.12) In Table A1 the analytical error, ϵ , is not given, page 21 line 6.

Thanks for noticing. We'll change the table A1 to:

	θ (°C)	S	SiO ₄ ($\mu\text{mol/kg}$)	NO ₃ ⁰ ($\mu\text{mol/kg}$)	PO ₄ ⁰ ($\mu\text{mol/kg}$)	O ₂ ^{0*} ($\mu\text{mol/kg}$)	TA ⁰ ($\mu\text{mol/kg}$)	DIC ⁿ _{SAT} ($\mu\text{mol/kg}$)	CDIS ($\mu\text{mol/kg}$)	CDIS ⁿ ($\mu\text{mol/kg}$)	Fractions uncertainties (%)
SWT _{STW16}	16 ± 0.06	35.1 ± 0.07	0.9 ± 0.2	1.2 ± 0.2	0.04 ± 0.3	243 ± 2	2290	1990	-19	1	0.04
SWT _{STW15}	15 ± 0.06	35.66 ± 0.07	0.6 ± 0.2	0 ± 0.2	0.12 ± 0.3	247 ± 2	2328	2026	-22	-2	0.04
SWT _{AASW}	-1.85 ± 0.006	33.8 ± 0.005	45 ± 2	30.7 ± 0.2	2.10 ± 0.3	360 ± 4	2289	2137	-23	-19	0.06
SWT _{SASW}	5 ± 0.008	33.8 ± 0.03	3 ± 0.2	23.3 ± 0.3	1.55 ± 0.5	310 ± 3	2264	2064	-13	-4	0.06
SWT _{HSSW}	-1.91 ± 0.08	34.71 ± 0.006	80 ± 1	28.3 ± 0.08	2.02 ± 0.03	300 ± 3	2351	2188	-21	0	0.08
SWT _{SAMW}	8.8 ± 0.02	34.63 ± 0.03	6 ± 0.6	13.2 ± 0.6	0.92 ± 0.8	280 ± 7	2290	2053	-10	2	0.03
SWT _{AAIW}	4 ± 0.01	34.35 ± 0.02	34 ± 2	29.2 ± 0.4	1.97 ± 0.9	220 ± 8	2299	2099	-16	-6	0.04
SWT _{NADW}	3.28 ± 0.008	34.91 ± 0.003	28 ± 1	27.5 ± 0.3	1.19 ± 0.7	220 ± 4	2355	2152	-27	-10	0.08
SWT _{CDW}	0.65 ± 0.006	34.707 ± 0.003	115 ± 7	30.8 ± 0.1	2.12 ± 0.1	220 ± 3	2351	2168	-23	-2	0.03
SWT _{PIDW}	1.44 ± 0.008	34.75 ± 0.005	125 ± 3	34.2 ± 0.01	3.4 ± 0.02	96 ± 2	2360	2168	-24	-4	0.04
SWT _{AABW}	-0.6 ± 0.006	34.66 ± 0.006	130 ± 5	30.7 ± 0.08	2.13 ± 0.03	259 ± 3	2355	2181	-22	-2	0.05
Weights	20	10	0.5	1	1	1					
SDR	0.004	0.003	6.0	0.50	0.04	2.0					
r²	0.99	0.99	0.98	0.99	0.99	0.99					

*Table A1. Properties of the SWTs characterizing the water masses of the SR03 section with the correspondent accuracies (ε). All SWTs are defined with preformed values of the variables (°). *The values of preformed oxygen (O₂⁰) are not in equilibrium for end members representing waters from the Antarctic shelf or old deep waters. The uncertainties in the fractions of the SWTs, the weights given to each variable in the OMP analysis, the Standard Deviation of the Residuals (SDR) and the square correlation coefficient (r²) between the observed values and the OMP estimates are also listed.*

- DIC changes: as suggested previously I suggest to start the methods sections with the proposed estimation of DIC changes and driving factors.

$$\Delta \text{DIC} = \Delta \text{DIC}^{\text{BIO}} + \Delta \text{DIC}^{\text{CANT}} + \Delta \text{DIC}^{\text{phys}}$$

please see Álvarez et al. (doi:10.1029/2010JC006475, 2011)

ΔDIC with your real measurements

$\Delta \text{DIC}^{\text{BIO}}$ will be computed as your Eq2, this term contains changes in mineralization

associated or not with changes in circulation / biology BUT correlated with AOU /

nutrients for sure. As you lack of transient tracers information you cannot account for changes in the transport, circulation independently.

$\Delta \text{DIC}^{\text{CANT}}$ with the OMP method (forget about the dis terms)

$\Delta \text{DIC}^{\text{phys}}$ as the difference between DIC- DIC^{CANT} - DIC^{BIO} , this term would contain any

changes in DIC not associated with AOU, mixing / Ventilation.... not accounted for in the CANT-OMP.

Following this methodology the blurred assumptions in page 8, lines 1 to 22 are avoid.

and of course I think it would help to explain the results.

We really thank you for the suggestion, however we consider that the proposed estimation of the DIC changes would not really allow us to avoid the lines in section 3.3, since somewhere we must address the issue of non-steady-state circulation and biological processes, and we believe the current paper structure is the best way to do this. As we mentioned before, we'll add some clarifications in the text at the beginning of the section (see answer to the point : “- circulation and biological processes at steady state”).

To respond specifically to your suggestions, the problem with using the proposed estimation of the change of DIC in the present manuscript is that:

- we have a range of values for $\Delta \text{DIC}^{\text{CANT}}$ (which corresponds to $\frac{\partial C_{\text{ANT}}}{\partial t}$ of the present manuscript)

- your recommended $\Delta \text{DIC}^{\text{phys}}$ is going to have as well a range of values that we will have to explain in the same way that we did with $\frac{\partial C_{\text{ANT_BC}}}{\partial t}$ and $\frac{\partial C_{\text{ANT}}}{\partial t}$. This may well create more confusion to the reader. That is why we think that adding the new text to the beginning of section 3.3 will help, since at the end of this additional text we'll mention that:

“The change in DIC not explained by these two quantities is due to circulation processes.” (see the complete text in the answer to the point : “- circulation and biological processes at steady state”).

Besides, in section 5 we discuss about the different drivers (solubility, biology or circulation) that are responsible for the change in DIC not explained by the change in C_{ANT} (see page 12 from line 9 to the end and lines 1-6 in page 13).

The use of the notation proposed in Álvarez et al. (doi:10.1029/2010JC006475, 2011) was good for their study. They use Transient tracer distributions (TTDs) to estimate C_{ANT} (TTDs rely on tracers to establish the amount of C_{ANT} in the deep ocean) and a numerical model to resolve the circulation effect on the AOU term. Thus, the terms with the different drivers affecting the variability of DIC were fully determined. The study was focussed on SAMW, which allowed for the TTD to give reliable values even using just one tracer (CFC-12), because the residence time of CFC-12 is efficient for waters of the age of SAMW. But this is not our situation, and we have previously explained why transient tracers are beyond the scope of this work.

I hope to have been helpful. Yes, of course. We thank you for your thorough review.

List of changes done to the manuscript:

- Correcting typos, text.
- Presentation of the supplementary material in a separate file from the main text.
- Addition of new text as a results of the comments from both reviewers
- Addition of tables and figures and correction of captions as a result of the comments from both reviewers.

Marked-up manuscript and marked-up supplementary material (blue highlight referring to reviewer-1 comments and green highlight for the changes referred to reviewer-2, see also the comments)

Carbon uptake and biogeochemical change in the Southern Ocean, south of Tasmania


Pardo, Paula C.¹, Tilbrook, Bronte^{1,2}, Langlais, Clothilde.², Trull, Tom W.^{1,2}, Rintoul, Steve R.^{1,2}

¹Antarctic Climate and Ecosystem Cooperative Research Centre, University of Tasmania, Hobart, Australia


²Climate Science Centre, CSIRO Oceans and Atmosphere, Hobart, Australia



Correspondence to: Paula C. Pardo (paula.condepardo@csiro.au)


Abstract. Biogeochemical change in the water masses of the Southern Ocean, south of Tasmania, was assessed for the 16-year period between 1995 and 2011 using data from 4 summer repeats of the WOCE/JGOFS/CLIVAR/GO-SHIP SR03 hydrographic section (at ~140°E). Changes in temperature, salinity, oxygen, and nutrients were used to disentangle the effect of solubility, biology, circulation and anthropogenic carbon (C_{ANT}) uptake on the variability of dissolved inorganic carbon (DIC) for 8 water mass layers defined by neutral surfaces (σ_θ). C_{ANT} was estimated using an improved back-calculation method. Warming ($\sim 0.0352 \pm 0.017$ °C yr⁻¹) of Subtropical Central Water (STCW) and Antarctic Surface Water (AASW) layers decreased their gas solubility, and accordingly DIC concentrations increased less rapidly than expected from equilibration with rising atmospheric CO₂ ($\sim 0.86 \pm 0.16$ μmol kg⁻¹ yr⁻¹ versus $\sim 1 \pm 0.12$ μmol kg⁻¹ yr⁻¹). An increase in apparent oxygen utilisation (AOU) occurred in these layers due to either remineralization of organic matter or intensification of upwelling. The range of estimates for the increases of C_{ANT} were 0.71 ± 0.08 to 0.93 ± 0.08 μmol kg⁻¹ yr⁻¹ for STCW and 0.35 ± 0.14 to 0.65 ± 0.21 μmol kg⁻¹ yr⁻¹ for AASW, with the lower values in each water mass obtained by assigning all the AOU change to remineralization. DIC increases in the Sub-Antarctic Mode Water (SAMW, 1.10 ± 0.14 μmol kg⁻¹ yr⁻¹) and Antarctic Intermediate Water (AAIW, 0.40 ± 0.15 μmol kg⁻¹ yr⁻¹) layers were similar to the calculated C_{ANT} trends. For SAMW, the C_{ANT} increase tracked rising atmospheric CO₂. As a consequence of the general DIC increase, decreases in total pH (pH_T) and aragonite saturation (Ω_{Ar}) were found in most water masses, with the upper ocean and the SAMW layer presenting the largest trends for pH_T decrease ($\sim -0.0031 \pm 0.0004$ yr⁻¹). DIC increases in deep and bottom layers ($\sim 0.24 \pm 0.04$ μmol kg⁻¹ yr⁻¹) resulted from the advection of old deep waters to resupply increased upwelling, as corroborated by increasing silicate ($\sim 0.21 \pm 0.07$ μmol kg⁻¹ yr⁻¹), which also reached the upper layers near the Antarctic Divergence ($\sim 0.36 \pm 0.06$ μmol kg⁻¹ yr⁻¹) and was accompanied by an increase in salinity. The observed changes in DIC over the 16-year span caused a shoaling (~ 340 m) of the aragonite saturation depth (ASD, $\Omega_{Ar} = 1$) within Upper

Circumpolar Deep Water that followed the upwelling path of this layer. From all our results, we conclude a scenario of increased transport of deep waters into the section and enhanced upwelling at high latitudes for the period between 1995 and 2011 linked  strong westerly winds. Although enhanced upwelling lowered the capacity of the AASW layer to uptake atmospheric CO₂, it did not limit that of the newly forming SAMW and AAIW, which exhibited C_{ANT} storage rates ($\sim 0.41 \pm 0.20 \text{ mol m}^{-2} \text{ yr}^{-1}$) twice that of the upper layers.

1 Introduction.

The Southern Ocean is a key region in terms of climate change and climate variability, influencing the Meridional Overturning Circulation and therefore modulating the global circulation and oceanic biogeochemical cycles (Sarmiento et al., 1998, 2004; Orr et al., 2005). Deep waters, formed in the North Atlantic, spread south and enter the Southern Ocean, where they mix with deep layers of the  arctic Circumpolar Current (ACC) and ultimately upwell between the Southern ACC Front and the Polar Front. The upwelled waters are eventually transformed into bottom, intermediate and mode waters, which are exported from the Southern Ocean to ventilate the thermocline and bottom layers of the major ocean basins. Some of the Southern Ocean waters subducted into the ocean interior return to the North Atlantic to balance the southward flux of North Atlantic Deep Water (Speer et al., 2000; Lumpkin and Speer, 2007; Iudicone et al., 2008).

 Within the eastward flow of the ACC major water exchange between the three ocean basins takes place. The circumpolar path of the ACC consists of various narrow jets associated with sharp fronts that separate waters with different characteristics (Orsi et al., 1995; Belkin and Gordon, 1996). These jets can reach deep layers and often meander, intensify, merge and split, conditioned by the topography of the ocean floor, the stratification of the ACC, and atmospheric variability (Moore et al., 1999; Sokolov and Rintoul, 2002, 2009; Peña-Molino et al., 2014). Movements in the jets enhance cross-stream transports and mesoscale activity that can result in local changes of water mass properties and  may complicate the computation of long-term changes in water mass properties (Rintoul and Bullister, 1999; Sallée et al., 2008; Peña-Molino et al., 2014).

Water mass formation and ventilation transport heat, salt, and dissolved gases from the atmosphere to the ocean interior and other basins (Sarmiento et al., 2004), with the Southern Ocean contributing $\sim 40\%$ to the anthropogenic CO₂ (C_{ANT}) inventory of the ocean  (Spence et al., 2004; Gruber et al., 2009; Khatiwala et al., 2009). Circulation and biological processes drive the redistribution of dissolved inorganic carbon (DIC) that ultimately affects the capacity of the waters to uptake more CO₂. The uptake of CO₂ by the Southern Ocean presents strong spatiotemporal variability (Lenton et al., 2013) and this can lead to conflicting results for observational studies, models and atmospheric inversions depending on the methodology used (Verdy et al., 2007; Lenton et al., 2012; Fay et al., 2014). Quantifying long-term changes in the carbon system is difficult due to the scarcity of data (Lenton et al., 2012; Kouketsu and Murata, 2014; Fay et al., 2014) and the influence of biological processes. Notably, long term trends in C_{ANT} concentration are difficult to estimate due to its small signal ($\sim 3\%$) with respect to that of DIC in the ocean.

Once CO₂ dissolves in the ocean (DIC) it begins the process of ocean acidification, i.e., decreases the pH and the saturation state of calcium carbonate (CaCO₃) minerals such as calcite and aragonite (Feely et al., 2004; Bates et al., 2014), with potential to disrupt ecosystems and biological processes (Doney et al., 2009).

Numerous studies have documented warming and freshening of deep and bottom layers of the Southern Ocean in recent decades (see reviews by Jacobs, 2006 and van Wijk and Rintoul, 2014). The abyssal waters of the Australian-Antarctic Basin (A-AB) show the greatest freshening in the last 40 years (van Wijk and Rintoul, 2014). This freshening was accompanied by a warming of the deep-bottom layers, leading to a contraction in bottom waters by more than half their volume in the basin (Purkey and Johnson, 2012; van Wijk and Rintoul, 2014). Subsurface to intermediate layers have also warmed and freshened south of Australia (Bindoff and Church, 1992; Wong et al., 1999; Aoki et al., 2005). The solubility of gases and its distribution in the ocean depends on the dynamics and properties of water masses, and the thermohaline changes that have occurred south of Tasmania (Fig. 1) have implications in the carbon system of the region.

A reduction of the carbon sink of the Southern Ocean was observed between the 1980s and the early 2000s (Le Quéré et al., 2007; Lovenduski et al., 2008), with more recent studies suggesting a recovery and even intensification of the CO₂ uptake by 2011-2012 (Zickfeld et al., 2008; Fay et al., 2014; Landschützer et al., 2015). DeVries et al. (2017), used a global inverse model to postulate that changes in circulation are responsible for most of the variability in the oceanic CO₂ uptake, with the weakening of the upper-ocean circulation being responsible for the increase in oceanic carbon uptake over the past decade. Ocean acidification has been observed in the whole Southern Ocean (Lauvset et al., 2015) and locally in the Atlantic and Pacific sectors (Williams et al., 2015; Hauri, et al., 2015). South of Tasmania, McNeil et al., (2001) reported an increase in C_{ANT} uptake between 1968 and 1996 for the region 45-50°S. These authors reported, for the first time, C_{ANT} accumulation in the AABW and highlighted the importance of the formation of bottom and mode waters as a mechanism for transporting C_{ANT} to the ocean. In terms of ocean acidification, we are not aware of any study about trends in ocean acidification in the water masses south of Australia.

Considering the lack of observational estimates for recent biogeochemical changes in the A-AB as well as the large changes in CO₂ uptake and storage suggested by recent atmospheric and surface observations in the Southern Ocean (e.g., Fay et al., 2014; Landschützer et al., 2015) there is a need to provide a full ocean depth observational perspective on how the ocean is changing. The aim of this paper is to provide the first estimates of biogeochemical change in the water masses south of Tasmania, for the period 1995-2011, disentangling the effects that solubility, circulation, biology and C_{ANT} uptake have on the variability of DIC. We use data from four summer repeats of the JGOFS/CLIVAR/GO-SHIP hydrographic section SR03 (Fig. 1; Table 1), one of the most revisited sections in the Southern Ocean. Trends in oxygen (O₂), nutrients, and the carbon system parameters, i.e., DIC, total alkalinity (TA), anthropogenic carbon (C_{ANT}), total pH (pH_T) and % aragonite saturation (Ω_{Ar}) were estimated for the period 1995-2011, when both DIC and TA measurements are available. C_{ANT} estimates were obtained with a back-calculation method (Pardo et al., 2014). The changes were evaluated in the different water mass layers of the section defined by neutral surfaces (γ_n, McDougall et al., 1987).

2 Hydrography of the region.

The dynamical structure of the region south of Tasmania (Fig. 1) is characterized by a number of fronts that separate the major water masses of the region (Sokolov and Rintoul 2002, 2007, 2009). At the northern end of the section, the presence of the weak Subtropical Front (STF, Fig. 1) separates warm, salty subtropical surface waters from cooler and fresher sub-Antarctic surface waters (Deacon, 1937). The northern end of the section is a complex mixing zone where waters transported down the east coast of Tasmania in a series of mesoscale eddies from the East Australian Current (EAC, Fig. 1) mix

into the Subantarctic Zone, and also meet Zeehan Current (ZC, Fig. 1) waters transported down the west coast of Tasmania (Boland and Church 1981; Baines et al., 1983; Speich et al., 2002; Davis, 2005; Ridgway et al., 2007; Sloyan et al., 2016). The EAC transported south of Tasmania forms a zonal jet towards the southeast Indian Ocean known as the Tasman Outflow that reaches the bottom of the Tasman slope and that is maintained all year round (Rintoul and Bullister, 1999; Ridgway et al., 2007). The encounter between these currents presents high variability at the northern end of the section (Fig. 1).

Farther south (Fig. 1), the Sub-Antarctic Front (SAF) and the Polar Front (PF) are regions of maximum transport in the ACC (Rintoul and Bullister, 1999; Sokolov and Rintoul 2002). North of the SAF, deep winter convection generates Sub-Antarctic Mode Water (SAMW), a relatively uniform water mass that occupies subsurface layers down to ~600m deep (McCartney, 1977; Rintoul and Bullister, 1999). SAMW constitutes the main part of the upper limb of the MOC, ventilating the thermocline of all the ocean basins (e.g., Speer et al., 2000; Sloyan and Rintoul, 2001). The SAF coincides with the deepening of the salinity minimum at intermediate depths (Whitworth and Nowlin, 1987), which is the signature of the Antarctic Intermediate Water (AAIW). The AAIW underlies the SAMW and also ventilates the global thermocline layers of the ocean. It is mainly formed in the southeast Pacific and it is continuously transformed on its way to the region south of Tasmania (Hanawa and Talley, 2001). South of the SAF, colder and fresher Antarctic Surface Water (AASW) covers the surface ocean. AASW originates from progressive warming of Winter Water (WW, Mosby, 1934), which can be perceived even in summer as a remnant layer of cold water at the base of the AASW (Rintoul et al. 1997).

The Southern ACC Front (SACCF, Fig. 1) is a deep front located south of the PF (Orsi et al., 1995) and can coincide with the southern boundary of the ACC, which is represented by the southern limit of the oxygen minimum (Orsi et al., 1995). The oxygen minimum is related to the advection of Upper Circumpolar Deep Water (UCDW) that originates in the Indian and Pacific Oceans (Callahan, 1972) from where it spreads south, mixes with deep layers of the ACC and ultimately upwells near the Antarctic continent as part of the lower cell of the MOC. Lower Circumpolar Deep Water (LCDW) is below UCDW and is identified by a salinity maximum and contributes to upwelling around Antarctica. The precursor of the LCDW is North Atlantic Deep Water (NADW), originated in the Labrador and Nordic seas of the North Atlantic polar region (Dickson and Brown, 1984) that flows southward to enter the ACC as part of the MOC (Callahan, 1972; Orsi et al., 1995; Johnson, 2008).

At the southern end of the section, the Antarctic Slope Front forms the boundary between cold and fresh shelf water and relatively warm and salty waters offshore (Jacobs, 1991). Polynyas along the Adélie and George V Land coast (Fig.1) contribute to the formation of Adélie Land Bottom Water (ALBW), which is a mixture of High Salinity Shelf Water (HSSW) resulting from brine rejection during ice formation and ultra-modified LCDW (Foster and Carmack, 1976; Rintoul, 1998; Marsland et al., 2004). ALBW constitutes ~ 25% of the total volume of water <0°C in the ocean (Rintoul, 1998). The bottom waters near the southern end of the section also contain a component of Ross Sea Bottom Water (RSBW) that originates to the east and is deflected westwards towards the A-AB as it is transported down the continental slope. The RSBW is modified when it arrives at the location of the SR03 section by mixing with deep layers of the ACC and recently formed ALBW (Gordon and Tchernia, 1972; Rintoul, 1998). The ALBW and the modified RSBW together ventilate the abyssal layers of the A-AB before spreading north to ventilate the Indian and Pacific basins (Mantyla and Reid, 1995; Fukamachi et al. 2010).

3 Data and Method.

3.1 Data.

The SR03 hydrographic section between Tasmania and Antarctica (Fig. 1) was occupied between 1991 and 2011. Measurements of total alkalinity (TA) were only available from the beginning of 1995 and our evaluation of biogeochemical changes is limited to four summer sections occupied for the period 1995-2011 (Table 1). A winter cruise in 1996 was not considered in this study in order to minimise seasonal biases.

Water column salinity, temperature, pressure and dissolved oxygen (O_2) were collected from the conductivity-temperature-depth (CTD) device with an accuracy of ± 0.002 for salinity and temperature, ± 0.015 % of full scale range for pressure and ± 1 % for O_2 , according to WOCE standards (Joyce, 1994). Samples from the Niskin bottles were analysed for dissolved inorganic carbon (DIC) by coulometry and TA by open cell potentiometric titration (Dickson et al, 2007). Certified reference material provided by Dickson, Scripps Institution of Oceanography, were used as reference standards for DIC and TA. The precisions of DIC and TA measurements improved slightly on more recent sections, and for all sections were better than $\pm 2 \mu\text{mol kg}^{-1}$, for both variables, based on analysis of duplicate samples and certified reference material. Samples for dissolved O_2 were measured using modified Winkler titrations (Hood et al 2010), with an estimated accuracy and precision of $\pm 0.3\%$ for the sections. For the 1995-cruise, sensor based O_2 was used instead of sampled O_2 because of the poor quality of many of the Winkler measurements.

Other variables of the dissolved CO_2 system were calculated from the DIC and TA measurements. We calculate pH_T and Ω_{Ar} (from measured DIC and TA) using the CO2sys program from Lewis and Wallace (1998) adapted to MATLAB by van Heuven et al. (2011). We use the constants for the carbonic acid from Mehrbach et al (1973) refit by Dickson and Millero (1987), the CO_2 solubility equation from Weiss (1974), dissociation constants for sulphate from Dickson (1990) and borate constant from Uppstrom (1974). Aragonite saturation states (Ω_{Ar}) are calculated because it is a less stable form of $CaCO_3$ than calcite and is the predominant biogenic form of $CaCO_3$ precipitated by calcifying organisms.


Data presented here were interpolated to a regular grid, and the water mass layers were defined as layers between neutral surfaces (σ^n) determined using potential temperature and salinity and published literature values (Table 2, section 2). The first 50m of the water column were eliminated in order to reduce the short-time scale variability in surface properties. The use of σ^n to identify the water mass layers reduces the variability due to isopycnal heave caused for example by eddies and internal waves (McDougall et al., 1987; Bindoff and McDougall, 1994; Jackett and McDougall, 1997). The upper ocean layers south of the SAF were divided into the AASW layer to the north of the PF, and the AASW_{upw} layer that is composed of surface waters south of the PF (Fig.1). ADLBW and RSBW were included in the AABW layer (Table 2). The ACC fronts along the SR03 section (Table 3) were defined as a function of hydrographic variables following Sokolov and Rintoul (2002).

3.2 Estimates of anthropogenic carbon (C_{ANT}).

C_{ANT} was estimated using a back-calculation method (Chen and Millero, 1979; Gruber, 1998) combined with an Optimum Multi-Parameter (OMP) analysis (Tomczak, 1981), described by Pardo et al. (2014). This technique has the advantage of considering water mass mixing and the temporal variability of the air-sea CO_2 disequilibrium. The accuracy of the method is $\pm 6 \mu\text{mol kg}^{-1}$ (Pardo et al., 2014). Back-calculation methods assume the ocean is in steady state for dynamical and biological processes and

estimate C_{ANT} (C_{ANT_BC}) as an excess of DIC in the ocean resulting from the increase of atmospheric CO_2 due to anthropogenic emissions as:

$$C_{ANT_BC} = DIC - DIC^{BIO} - DIC^{\pi} \quad (1)$$


where DIC^{BIO} is the biological contribution to DIC, and DIC^{π} is  concentration of DIC in preindustrial times.

The term DIC^{BIO} , is calculated (Chen et al., 1982; Ikegami and Kanamori, 1983) by:

$$DIC^{BIO} = \frac{AOU}{R_C} + \frac{1}{2} \left[TA - TA^0 + AOU * \left(\frac{1}{R_N} + \frac{1}{R_P} \right) \right] \quad (2)$$

where R_C , R_N and R_P are the stoichiometric ratios of carbon, nitrate and phosphate respectively, referred to O_2 consumption by respiration/remineralization processes that are considered constant (1.45, 9, 125, respectively, Broecker, 1974; Anderson and Sarmiento, 1994; Martiny et al., 2013).

$\frac{AOU}{R_C}$ represents the remineralization of organic matter, with the apparent oxygen utilization (AOU) defined as ($AOU = O_{SAT} - O_2$) the difference between the saturation of oxygen (O_{SAT}) at the potential temperature (θ) and salinity of the measured O_2 . The term $\frac{1}{2} \left[TA - TA^0 + AOU * \left(\frac{1}{R_N} + \frac{1}{R_P} \right) \right]$, represents the dissolution/precipitation of $CaCO_3$, with TA^0 , the preformed alkalinity, obtained in the water formation sites using regional parameterizations as function of salinity, θ and phosphate (Pardo et al., 2011; Vázquez-Rodríguez et al., 2012; Appendix section A3, Table A3).

The  preindustrial term, DIC^{π} , is the total concentration of carbon dioxide in seawater saturated with respect to the preindustrial pCO_2 (DIC_{SAT}^{π}) and corrected for an air-sea CO_2 disequilibrium ($CDIS^{\pi}$) term:

$$\text{formed}^{\pi} = DIC_{SAT}^{\pi} + CDIS^{\pi} \quad (3)$$

$CDIS^{\pi}$ is time dependent:

$$CDIS^{\pi} = CDIS - \delta CDIS \quad (4)$$

where $CDIS$ is the current disequilibrium between the ocean and the atmosphere pCO_2 , and $\delta CDIS$ is the change in the disequilibrium from preindustrial to current times. $CDIS$ was obtained by similar parameterizations to those used for TA^0 , combined with monthly mean values of atmospheric CO_2 values from the NOAA network (Dlugokencky, et al., 2016) (see section A3 of the appendix and Table A3). The $\delta CDIS$ values were obtained from results of the $1/10^\circ$ resolution carbon model OFAM3-WOMBAT (Appendix section A1).

Interior values of preformed variables (TA^0 and DIC_{SAT}^{π}) and $CDIS^{\pi}$ were obtained using an optimum multiparameter (OMP) analysis to mix end members as described in Appendix sections A2 and A3, using the end members in Table A1. The OMP analysis is based on the assumption that a property measured in a certain point is the result of linear mixing between end members, known as source water types (SWTs). A system of equations is created for each measurement point and is solved to obtain the fractions of the different SWTs (Appendix section A2). The application of the OMP analysis requires good regional hydrodynamic knowledge as the results are strongly dependant on the definition of the SWTs (Tomczak, 1981). We used 11 SWTs to characterize the biogeochemical properties of the waters in the SR03 section and the SWT properties were assumed to be constant with time (Appendix Table A1, Fig. A1).

Small negative values of C_{ANT_BC} can occur due to an overestimation of the $CDIS^\pi$ term (Eq. 4), that acts as measure of the age of the water mass and has high values in old deep layers (see Table A1 in the appendix). These negative values of C_{ANT_BC} were found at some points in deep waters of the section (mainly UCDW and LCDW layers) and were small (between 0 and $-2 \mu\text{mol kg}^{-1}$, i.e., less than the accuracy of the methodology) and changed to zero for our analysis.

3.3 Changes in the carbon system.

Changes in carbon system parameters ($\frac{\partial DIC}{\partial t}$, $\frac{\partial TA}{\partial t}$, $\frac{\partial C_{ANT_BC}}{\partial t}$, $\frac{\partial pH}{\partial t}$ and $\frac{\partial \Omega_{Ar}}{\partial t}$) were estimated using linear regressions with time for the period 1995-2011 in each one of the water mass layers defined by their σ_θ condition (Table 2). The trends were estimated using all the points in each water mass layer and only those linear trends with $p < 0.05$ and $r \geq 0.2$ were considered statistically significant for discussion.

show the value of the root mean square error (RMSE or square root of the variance of the residuals), which can be interpreted in large part as unexplained variance caused by short-time scale processes and the different seasonal timings of the cruises. RMSE has the same units as the response variable.

With respect to the total change of DIC ($\frac{\partial DIC}{\partial t}$), our goal is to disentangle the effects that solubility, circulation, biology and C_{ANT} uptake have on the variability of DIC. The total change of DIC ($\frac{\partial DIC}{\partial t}$) in a water mass is due to changes in the atmosphere-ocean interchange, biological processes and circulation processes. In order to account of the change in DIC due the atmosphere-ocean interchange and biological processes, we compare $\frac{\partial DIC}{\partial t}$ to $\frac{\partial C_{ANT_BC}}{\partial t}$ and $\frac{\partial DIC^{BIO}}{\partial t}$, Eq. (2). The change in DIC not explained by $\frac{\partial C_{ANT_BC}}{\partial t}$ or $\frac{\partial DIC^{BIO}}{\partial t}$ will then be due to circulation processes.

In order to compare $\frac{\partial DIC}{\partial t}$ to $\frac{\partial C_{ANT_BC}}{\partial t}$ we need to consider how the change in $\frac{\partial DIC^{BIO}}{\partial t}$ and DIC^π ($\frac{\partial DIC^\pi}{\partial t}$) (terms of Eq (1), section 3.2) affect the changes in C_{ANT_BC} . The term $\frac{\partial DIC^\pi}{\partial t}$ can be expressed as:

$$\frac{\partial DIC^\pi}{\partial t} = \frac{\partial DIC_{SAT}^\pi}{\partial t} - \frac{\partial CDIS^\pi}{\partial t} \quad (5)$$

The terms $\frac{\partial CDIS^\pi}{\partial t}$ and $\frac{\partial DIC_{SAT}^\pi}{\partial t}$ reflect changes in the properties of the water masses over time, primarily temperature and salinity change due to mixing and heating/cooling. $CDIS^\pi$ and DIC_{SAT}^π are defined at the ocean surface (in each of the SWTs: Table A1) and are calculated at each point in the ocean interior using the OMP analysis (Appendix sections A2 and A3). Because a change in temperature and/or salinity in the water is solved by the OMP analysis as a change in the SWTs fractions, this also produces varying $CDIS^\pi$ and DIC_{SAT}^π . No significant trends were obtained for $CDIS^\pi$ in any of the layers. C_{ANT_BC} (Eq. 1) is not affected by the changes in solubility occurring from one voyage to another (thus neither is $\frac{\partial C_{ANT_BC}}{\partial t}$), since any change in temperature or salinity is cancelled out by the subtraction of DIC^π with respect to DIC in Eq. (1) (section 3.2) and by O_2 respect to O_{SAT} in the DIC^{BIO} term (Eq. 2). However, $\frac{\partial DIC}{\partial t}$ based on the measured DIC in the sections will be affected by changes in the solubility over time and this difference needs to be accounted for when comparing $\frac{\partial DIC}{\partial t}$ with $\frac{\partial C_{ANT_BC}}{\partial t}$ to obtain a better approximation for the change in C_{ANT} : $\frac{\partial C_{ANT}}{\partial t} = \frac{\partial C_{ANT_BC}}{\partial t} + \frac{\partial DIC^\pi}{\partial t}$.

The term $\frac{\partial DIC^{BIO}}{\partial t}$ can be influenced by changes with time of alkalinity due to changes in the rate of carbonate precipitation/dissolution and of AOU due to changes in the rate of remineralization and in circulation. In the present study only surface waters of the SR03 section present changes DIC^{BIO} between 1995 and 2011. Numerous studies have reported a strong influence of biological communities in the seasonal cycle of dissolved O_2 in surface waters (Bender et al., 1996; Moore and Abbott, 2000; Sambrotto and Mace, 2000; Trull et al., 2001a). Interannual variability in O_2 in upper layers of the Southern Ocean have also been related to changes in the entrainment of deeper waters into the mixed layer due to the mixed layer depth variability (Matear et al., 2000; Verdy et al., 2007; Line et al., 2008; Sallée et al., 2012). Although some studies found long-term decreases in O_2 due to circulation in deep waters of the Weddell Sea (van Heuven et al., 2014) and for the first 1000 m of the global ocean (Helm et al. 2011), significant long-term trends in O_2 due to circulation and remineralization processes have not yet been reported for surface waters of the Southern Ocean. Thus, the term $\frac{\partial DIC^{BIO}}{\partial t}$ may also contribute to variation in $\frac{\partial C_{ANT-BC}}{\partial t}$, since part of the changes in AOU with time reflect changes in circulation that we cannot separate from those in remineralization. We consider the best approximation for the change in C_{ANT} as a range depending on the possible effect of biology and circulation processes on $\frac{\partial DIC^{BIO}}{\partial t}$. If the value of $\frac{\partial DIC^{BIO}}{\partial t}$ is due to the variability in the remineralization rates and the change in solubility is considered, the estimate $\frac{\partial C_{ANT-BC}}{\partial t}$ will be the lower limit of the range, (lower limit of $\frac{\partial C_{ANT}}{\partial t} = \frac{\partial C_{ANT-BC}}{\partial t} + \frac{\partial DIC^{\pi}}{\partial t}$). For the upper limit of the range, we consider that the value of $\frac{\partial DIC^{BIO}}{\partial t}$ is due to changes in circulation and the upper limit of the range is obtained by $\frac{\partial C_{ANT}}{\partial t} = \frac{\partial C_{ANT-BC}}{\partial t} + \frac{\partial DIC^{\pi}}{\partial t} + \frac{\partial DIC^{BIO}}{\partial t}$ (see schematic accompanying table 5). We assume that the changes in DIC^{BIO} due to circulation do not affect the amount of DIC in the layer. This assumption is one of the caveats of the methodology, since we cannot know how much of the change in DIC is associated to changes in circulation, i.e., how much of the change in DIC is a change in non-anthropogenic DIC. We will discuss this more in section 4.

4 Results.

The different trends in biogeochemical properties are summarized in Table 4. The biogeochemical changes between 1995 and 2011 are presented for each of the water mass layers and the effect of changes in solubility, biological processes and circulation in the estimates of $\frac{\partial C_{ANT}}{\partial t}$ and $\frac{\partial DIC}{\partial t}$ are considered along with changes in the aragonite saturation depth and C_{ANT} storage.

4.1 Changes in DIC, C_{ANT} and pH_T (1995-2011).

4.1.1 Upper ocean layers (STCW, AASW and AASW_{upw}).

In the STCW layer, DIC increased between 1995 and 2011 (Fig. 2a, b) at a rate of $0.86 \pm 0.07 \mu\text{mol kg}^{-1} \text{yr}^{-1}$ ($\frac{\partial DIC}{\partial t}$, Table 4), leading to a decrease of pH_T of $-0.0027 \pm 0.0001 \text{yr}^{-1}$ ($\frac{\partial pH_T}{\partial t}$, Table 4, Fig. 2e, f). The trend in pH_T is similar to the one found by Lauvset et al. (2015) between 1991 and 2011 for the IO-STPS (Indian Ocean subtropical permanently stratified) biome ($-0.0027 \pm 0.0005 \text{yr}^{-1}$). We found a decrease of DIC^{π} ($\frac{\partial DIC^{\pi}}{\partial t} = -0.34 \pm 0.06 \mu\text{mol kg}^{-1} \text{yr}^{-1}$, Table 5) in the STCW layer due to a negative trend of DIC_{SAT}^{π} resulting from a decrease in solubility that resulted from a temperature increase

(calculated from the section data) in the STCW layer of $0.0335 \pm 0.0130 \text{ } ^\circ\text{C yr}^{-1}$ (not shown). The increase in temperature agrees with the warming trend observed south of Tasmania of 0.2 to 0.3 $^\circ\text{C decade}^{-1}$ obtained from satellite data (Armour and Bitz, 2015) and from combined data and models ($0.5 \text{ } ^\circ\text{C} / 30 \text{ yr}^{-1}$, Aoki et al., 2015). For $\theta=16 \text{ } ^\circ\text{C}$ and $S=35.1$ (definition of $\text{SWT}_{\text{STW16}}$ in the OMP analysis, Table A1), a change in temperature of $0.03 \text{ } ^\circ\text{C yr}^{-1}$ would lead to a decrease in $\text{DIC}_{\text{SAT}}^\pi$ of $-0.27 \text{ } \mu\text{mol kg}^{-1} \text{ yr}^{-1}$, which is similar to the value obtained for $\frac{\partial \text{DIC}^\pi}{\partial t}$ in the STCW layer (Table 5). The difference between these trends is related to the mixing of the different SWTs fractions within the STCW layer established from the OMP analysis (see section 3 and section A2 of the Appendix). When the solubility change is incorporated into $\frac{\partial C_{\text{ANT-BC}}}{\partial t}$, i.e. $\frac{\partial C_{\text{ANT-BC}}}{\partial t} + \frac{\partial \text{DIC}^\pi}{\partial t}$ (Table 5, Fig. 2c, d), we obtain a value of $0.71 \pm 0.08 \text{ } \mu\text{mol kg}^{-1} \text{ yr}^{-1}$.

There is an increase of DIC^{BIO} in the STCW layer ($\frac{\partial \text{DIC}^{\text{BIO}}}{\partial t}$, Table 5), that also affects the estimates of $\frac{\partial C_{\text{ANT-BC}}}{\partial t}$. The increase of DIC^{BIO} is due to an increase in AOU (no changes were found in TA, Eq. (2) in section 3.2) due to a decrease of O_2 in the layer. We cannot separate the effects of circulation and biology on the AOU change and $\frac{\partial C_{\text{ANT}}}{\partial t}$ in Table 4 should be considered a range. If the changes in AOU are only due to the variability in the remineralization rates, the calculated lower limit of $\frac{\partial C_{\text{ANT}}}{\partial t}$ is $0.71 \pm 0.08 \text{ } \mu\text{mol kg}^{-1} \text{ yr}^{-1}$ (Table 4, $\frac{\partial C_{\text{ANT}}}{\partial t} = \frac{\partial C_{\text{ANT-BC}}}{\partial t} + \frac{\partial \text{DIC}^\pi}{\partial t}$ in Table 5). If the changes in AOU are due to changes in circulation, the upper limit value of $0.93 \pm 0.11 \text{ } \mu\text{mol kg}^{-1} \text{ yr}^{-1}$ ($\frac{\partial C_{\text{ANT}}}{\partial t} = \frac{\partial C_{\text{ANT-BC}}}{\partial t} + \frac{\partial \text{DIC}^\pi}{\partial t} + \frac{\partial \text{DIC}^{\text{BIO}}}{\partial t}$) will explain the increase of DIC in the STCW layer ($\frac{\partial \text{DIC}}{\partial t} \approx \frac{\partial C_{\text{ANT}}}{\partial t}$, Table 4). The increase of C_{ANT} found in this layer is comparable to the range of increase ($0.8 - 1.3 \text{ } \mu\text{mol kg}^{-1} \text{ yr}^{-1}$) found by Carter et al. (2017) in the Pacific Ocean (P16 WOCE, CLIVAR and GOSHIP lines) for the two past decades (1990s-2000s and 2000s-2010s).

Changes in the AASW layer are summarised in Table 4. DIC increased at a similar rate of $0.85 \pm 0.14 \text{ } \mu\text{mol kg}^{-1} \text{ yr}^{-1}$ to the STCW layer and the trend is similar to the values found by Williams et al. (2015) for the AASW layer in the Pacific sector of the SO ($12\text{-}18 \text{ } \mu\text{mol kg}^{-1}$ for the period 1992-2011 and $3\text{-}5 \text{ } \mu\text{mol kg}^{-1}$ for the period 2005-2011). The increase of DIC in the AASW layer results in a pH_τ decrease of $-0.0035 \pm 0.0002 \text{ yr}^{-1}$, close to Williams et al. (2015) estimates for surface waters ($\sim -0.0023 \pm 0.0009 \text{ yr}^{-1}$) and Lauvset et al. (2015) estimates of $-0.0021 \pm 0.0002 \text{ yr}^{-1}$ for the Southern Ocean seasonally stratified, SO-SPSS, biome. The AASW layer for our sections warmed at a similar rate ($0.0369 \pm 0.0109 \text{ } ^\circ\text{C yr}^{-1}$) to the STCW layer, reducing the solubility and influencing $\frac{\partial \text{DIC}^\pi}{\partial t}$ (Table 5) due to changes in $\text{DIC}_{\text{SAT}}^\pi$. The DIC^{BIO} also increased with time ($0.50 \pm 0.16 \text{ } \mu\text{mol kg}^{-1} \text{ yr}^{-1}$, Table 5) due to an increase of AOU. Following the same reasoning as for the STCW layer and considering the trend in C_{ANT} of $0.70 \pm 0.06 \text{ } \mu\text{mol kg}^{-1} \text{ yr}^{-1}$ obtained by the back-calculation method ($\frac{\partial C_{\text{ANT-BC}}}{\partial t}$; Table 5), the best estimation of $\frac{\partial C_{\text{ANT}}}{\partial t}$ in the AASW layer is a range of 0.35 ± 0.14 to $0.85 \pm 0.22 \text{ } \mu\text{mol kg}^{-1} \text{ yr}^{-1}$ (Table 4). Our values are within the range of values found by Williams et al. (2015) for the AASW in the Pacific sector between 2005 and 2011 and the upper limit is similar to a C_{ANT} increase of $0.73 - 0.86 \text{ } \mu\text{mol kg}^{-1} \text{ yr}^{-1}$ for waters South of Tasmania for the period 1968-1996 found by McNeil et al. (2001).

DIC in the AASW_{upw} layer increased at a rate of $0.61 \pm 0.10 \text{ } \mu\text{mol kg}^{-1} \text{ yr}^{-1}$, and the pH_τ decreased $-0.0015 \pm 0.0004 \text{ yr}^{-1}$ (Table 4). We were not able to detect a statistically significant trend in DIC^π (i.e., solubility) or C_{ANT} from the estimates of the back-calculation method ($\frac{\partial C_{\text{ANT-BC}}}{\partial t}$ Table 5). However, we found an increase of DIC^{BIO} of $0.42 \pm 0.28 \text{ } \mu\text{mol kg}^{-1} \text{ yr}^{-1}$ (Table 5) that is due to an increase in AOU.

Considering the different drivers of the AOU increase (biology/circulation), the optimal estimation of $\frac{\partial C_{ANT}}{\partial t}$ for this layer is a value between 0 and $0.42 \pm 0.28 \mu\text{mol kg}^{-1} \text{yr}^{-1}$ (Table 4).

4.1.2 Mode waters and intermediate layers (SAMW and AAIW).

The increase in DIC in the SAMW layer ($1.10 \pm 0.14 \mu\text{mol kg}^{-1} \text{yr}^{-1}$) for the period 1995-2011 is higher than that of upper ocean layers and pH_T decreases over the same period at $-0.0031 \pm 0.0003 \text{yr}^{-1}$ (Table 4). The DIC increase is explained almost entirely by $\frac{\partial C_{ANT_BC}}{\partial t}$ of $0.92 \pm 0.09 \mu\text{mol kg}^{-1} \text{yr}^{-1}$. No significant trend was found in DIC^{BIO} or DIC^π (i.e., $\frac{\partial C_{ANT}}{\partial t} = \frac{\partial C_{ANT_BC}}{\partial t}$). In the AAIW layer the DIC trend of $0.40 \pm 0.15 \mu\text{mol kg}^{-1} \text{yr}^{-1}$ results in a pH_T decrease of $-0.0017 \pm 0.0002 \text{yr}^{-1}$ and is also explained by the increase of C_{ANT} ($0.42 \pm 0.06 \mu\text{mol kg}^{-1} \text{yr}^{-1}$, $\frac{\partial C_{ANT}}{\partial t} = \frac{\partial C_{ANT_BC}}{\partial t}$, Tables 4 and 5). As with SAMW, no changes in solubility ($\frac{\partial \text{DIC}^\pi}{\partial t}$) or biology/circulation processes ($\frac{\partial \text{DIC}^{BIO}}{\partial t}$) were detected in the AAIW layer. The values found in the SAMW and AAIW layers are very similar to the mean decadal changes found by Murata et al. (2007) between the 1990s and the 2000s in the subtropical Pacific Ocean ($\sim 1 \mu\text{mol kg}^{-1} \text{yr}^{-1}$ for the SAMW layer and $0.4 \mu\text{mol kg}^{-1} \text{yr}^{-1}$ for the AAIW). Waters et al., (2011) used data from the P18 line along $\sim 110^\circ\text{W}$ and estimated an increase in C_{ANT} of $0.89 \pm 0.4 \mu\text{mol kg}^{-1} \text{yr}^{-1}$ for the SAMW and $0.64 \pm 0.2 \mu\text{mol kg}^{-1} \text{yr}^{-1}$ in AAIW for the period 1994-2008, which are also comparable to our results.

4.1.3 Deep-bottom layers (UCDW, LCDW and AABW).

The UCDW layer shows an increase of DIC of $0.29 \pm 0.02 \mu\text{mol kg}^{-1} \text{yr}^{-1}$ between 1995 and 2011 and a change in pH_T of $-0.0013 \pm 0.0001 \text{yr}^{-1}$ and are similar to the change in DIC ($0.20 \pm 0.02 \mu\text{mol kg}^{-1} \text{yr}^{-1}$) and pH_T ($-0.0012 \pm 0.0002 \text{yr}^{-1}$) for LCDW. No statistically significant changes in time were detected of C_{ANT_BC} or in the DIC^{BIO} and DIC^π terms for any of these two layers.

The AABW layer also shows an increase of DIC ($0.24 \pm 0.02 \mu\text{mol kg}^{-1} \text{yr}^{-1}$) during the period 1995-2011 with an associated decrease of pH_T of $-0.0013 \pm 0.0002 \text{yr}^{-1}$ (Table 4). The increase in C_{ANT} ($\frac{\partial C_{ANT_BC}}{\partial t}$) of $0.07 \pm 0.01 \mu\text{mol kg}^{-1} \text{yr}^{-1}$ is low and this trend indicates an increase in C_{ANT} of $\sim 1 \mu\text{mol kg}^{-1}$, which is less than the accuracy of the back-calculation method ($\pm 6 \mu\text{mol kg}^{-1}$).

4.2 Changes in the aragonite saturation ($\frac{\partial \Omega_{Ar}}{\partial t}$) and C_{ANT} storage.

There are statistically significant decreases of Ω_{Ar} in the STCW, AASW and SAMW layers ($\sim -0.010 \pm 0.001 \text{yr}^{-1}$, Table 4) similar to the trends observed at open-ocean time series sites in recent decades (Bates et al., 2014). The decrease of Ω_{Ar} found for the AASW layer ($-0.61 \pm 0.19 \% \text{yr}^{-1}$, Table 4) is also similar to the values obtained by Williams et al. (2015) for the Pacific sector of the Southern Ocean ($-0.47 \pm 0.10 \% \text{yr}^{-1}$ for the period 1992 -2011 and $-0.50 \pm 0.20 \% \text{yr}^{-1}$ for the period 2005-2011). Accompanying the decrease of Ω_{Ar} with time along SR03, is the shoaling of the aragonite saturation depth (ASD, $\Omega_{Ar} = 1$, Fig. 3) at a mean rate of $-13 \pm 3 \text{m yr}^{-1}$. The shoaling of the ASD is not uniform over the section. North of the PF, the ASD shoals at a rate of $-6 \pm 4 \text{m yr}^{-1}$ while the rate is 3.5 times greater south of the PF ($-21 \pm 4 \text{m yr}^{-1}$). North of the PF the shoaling mostly affects the AAIW layer (Fig. 3a). South of the PF from $\sim 62^\circ\text{S}$, the movement of the ASD follows the upwelling path of the UCDW layer (Fig. 3) with a shoaling of $\sim 340 \text{m}$ over the 16-year period.

The storage rate of C_{ANT} (Table 6) for the surface and intermediate water mass layers is obtained from $\frac{\partial C_{ANT}}{\partial t}$ (Table 4) with the most storage in SAMW and AAIW due to both their greater thickness and

$\frac{\partial C_{ANT}}{\partial t}$ values. The rate of increase of the C_{ANT} storage in the whole longitude band of the SR03 section is $0.30 \pm 0.24 \text{ mol m}^{-2} \text{ yr}^{-1}$, calculated by computing the mean of the storage rates of the layers weighted by the mean volume occupied by each of the layers for the period 1995-2011 (Table 6)

5 Discussion.

Our results are indicative of a scenario of increased transport of deep waters into the section and enhanced upwelling at high latitudes for the period between 1995 and 2011 linked to strong westerly winds. Several studies have reported a trend in the Southern Annular Mode (SAM) toward its positive phase from the 1960s until the 2000s (Thompson and Solomon, 2002; Marshall, 2002, 2003; Lenton and Matear, 2007; Sallée et al., 2008). According to these studies, the positive phase of the SAM is correlated with an intensification and southward movement of the subpolar westerly winds that ultimately lead to the enhancement of northward Ekman transport, meridional overturning and upwelling south of the ACC. Also, surface warming and more intense and frequent pulses in the extension of the EAC at long-time scales have been related to a poleward movement of the westerly winds (Rintoul and Sokolov, 2001; Ridgway, 2007; Hill et al., 2011). From the 2000s on, the SAM index no longer presents a positive trend but, although exhibiting considerable interannual variability (Fig. A2 in the supplementary material), the SAM index remains in its positive phase, favouring strong winds over the region.

In the northern part of the SR03 section, the area occupied by the STCW has high variability due to the encounter between the EAC and the ZC in the North of the section (Ridgway et al., 2007; Herraiz-Borreguero and Rintoul, 2011; Sloyan et al., 2016). The warming of the STCW layer found in this study ($0.0335 \pm 0.0130 \text{ }^{\circ}\text{C yr}^{-1}$) could be linked to variability in the extension of subtropical waters but it could also be related to atmospheric warming. Aoki et al. (2015) related the 30-year warming found north of the SAF in the South Pacific and Indian oceans to the intensification of the subtropical gyres, which promote the arrival of warmer waters. In the AASW layer that extends approximately between the SAF and the PF we found a similar warming ($0.0369 \pm 0.0109 \text{ }^{\circ}\text{C yr}^{-1}$) to that of the STCW. This could indicate that the increase of temperature found in the upper layers of the section could be most likely due to ocean heat uptake and atmosphere warming.


Due to the surface warming, the increase of DIC found in the STCW layer (Table 4) is lower than expected from the increase in atmospheric CO_2 ($\sim 1 \pm 0.12 \text{ } \mu\text{mol kg}^{-1} \text{ yr}^{-1}$). Nevertheless, at least 83% of the increase of DIC in the STCW layer is explained by the increase in C_{ANT} (Table 4). As for the AASW layer, our results indicate that temperature does affect the estimate of $\frac{\partial DIC}{\partial t}$, but the effect of the increase in DIC^{Bio} (due to an increase in AOU) overweigh that of solubility (Table 5).

The seasonal to interannual variability of the AASW layer is also influenced by the variability of the positions of the SAF and PF (Fig. 1, Table 3), that is highly conditioned by the flow of the ACC over the South-East Indian Ridge (Fig. 1). A close relationship between phytoplankton blooms and regions where the ACC fronts interact with large topographic features has been noticed (Moore et al., 1999; Moore and Abbott, 2000). A variability in the remineralization rates due to phytoplankton blooms variability could explain the changes in DIC^{Bio} observed in the AASW layer. Nevertheless, no changes in nutrients (nitrates or phosphates) are measurable in this layer that could indicate intense biological activity.

Furthermore, the AASW layer is also affected by the upwelling of deep waters south of the PF, and an intensification of the upwelling could increase the content of low- O_2 DIC-rich waters in the AASW layer

leading to an increase in AOU. The increase in DIC^{BIO} found in the AASW_{upw} layer (Table 4), south of the PF, is similar to the increase obtained for the AASW layer, which indicates the likelihood that the upwelling of deep waters results in the increase in AOU. The increase in DIC^{BIO} in the AASW_{upw} layer coincides with an increase of salinity of $0.0029 \pm 0.0001 \text{ yr}^{-1}$ (not shown), that is consistent with increased transport of saltier waters from the deep ocean to subsurface layers. Besides, we also found an increase in dissolved silicate of $0.36 \pm 0.06 \mu\text{mol kg}^{-1} \text{ yr}^{-1}$ ($\frac{\partial SiO_4}{\partial t}$ Table 4) that could be related to the upwelling enhancement as well (Tréguer, 2014).

The influence of the upwelling on the DIC budgets (as non-anthropogenic DIC) is clearer in the AASW_{upw} layer than in the AASW layer. For the AASW layer, the lower limit of $\frac{\partial C_{ANT}}{\partial t}$ (i.e., the change in DIC^{BIO} is assumed to be due to biological processes, Table 4) indicates that at least 41% of the increase of DIC in the layer is explained by the increase of C_{ANT} while the lower limit of $\frac{\partial C_{ANT}}{\partial t}$ is zero for AASW_{upw} (Table 4), meaning that the effect of the upwelling over AASW is lower than over AASW_{upw}. Matear and Lenton (2008) using carbon models, concluded that the uptake of CO_2 by the waters north of the PF is more influenced by the wind variability than by other processes such as the upwelling. An intensification of the winds (due to a positive phase in SAM) could contribute to the increase in C_{ANT} found in the AASW layer. Considering the upper limits of $\frac{\partial C_{ANT}}{\partial t}$ in both layers (i.e., the change in DIC^{BIO} is assumed to be due to circulation processes), the increase of C_{ANT} in the AASW_{upw} layer represents no more than 69% of the increase in DIC (upper limit of $\frac{\partial C_{ANT}}{\partial t}$, Table 4) while the upper limit of $\frac{\partial C_{ANT}}{\partial t}$ for the AASW equals the increase of DIC. Thus, AASW_{upw} layer, at least ~30% of the increase in DIC ($\sim 0.18 \mu\text{mol kg}^{-1} \text{ yr}^{-1}$) is still not explained and is most probably related to the upwelling of DIC-rich waters. The increase in non-anthropogenic DIC could be even higher, since we assume that the change in DIC^{BIO} due to circulation does not affect DIC (see section 3.3).

 In terms of the change in oxygen, Helm et al. (2011) found an average decrease in the concentration of O_2 between 100 and 1000 m from 1970 to 1992 of $\sim -0.23 \mu\text{mol l}^{-1}$ for the Southern Ocean (27% of the estimated global average change, $-0.93 \pm 0.23 \mu\text{mol l}^{-1}$). Considering the volume of the first 1000 m of the water column of the Southern Ocean to be $19400 \cdot 10^9 \text{ l}$ (obtained using ETOPO1 doi:10.7289/V5C8276M) and the volume of the first 1000 m of the SR03 section to be $2700 \cdot 10^9 \text{ l}$, the decrease of O_2 found by Helm et al. (2011), if constant in time, would correspond to a decrease of $\sim -1.7 \mu\text{mol l}^{-1} \text{ yr}^{-1}$. We only found changes in oxygen within the surface water mass layers (STCW, AASW and AASW_{upw}) that approximately fill the first 300 m of the water column of the SR03. Then, the decrease of $\sim -1.7 \mu\text{mol l}^{-1}$ would correspond to an average change of O_2 of $\sim -0.32 \mu\text{mol kg}^{-1} \text{ yr}^{-1}$ for surface waters of the SR03. This means that values of $\sim 0.20 \mu\text{mol kg}^{-1} \text{ yr}^{-1}$ due to circulation processes can be expected in $\frac{\partial DIC^{BIO}}{\partial t}$ for surface waters, which is comparable to the average of our findings (Table 5), $0.32 \pm 0.24 \mu\text{mol kg}^{-1} \text{ yr}^{-1}$ and could indicate that the change in O_2 is related to circulation processes.

The variability of the SAMW and AAIW layers south of Tasmania has been related to variability in the northward Ekman transport that drives the northward movement of AASW (Rintoul and England, 2002; Sallée et al., 2006, 2012). A scenario of intensification of the upwelling near the Antarctic Divergence would lead to an increase in the northward Ekman transport, conditioning the properties of these water mass layers and particularly for SAMW, which is mostly from north of the SAF. There is a significant freshening of the SAMW layer ($-0.0026 \pm 0.0001 \text{ psu yr}^{-1}$, not shown) between 1995 and 2011 that could be related to higher inputs of AASW into the SAMW layer and consistent with the increase in Ekman transport. Besides, an intensification of the winds due to the positive trend of the

SAM favours the ventilation and thus the increase in C_{ANT} uptake by both water mass layers (Matear and Lenton, 2008). Our results indicate that the change of DIC in the SAMW and AAIW layers is driven mostly by the uptake of atmospheric CO_2 ($\frac{\partial DIC}{\partial t} \approx \frac{\partial C_{ANT}}{\partial t}$, Table 4). The increase of C_{ANT} in the SAMW layer is higher than that found for the upper ocean layers and closer to the expected from the increase of atmospheric CO_2 ($\sim 1 \mu\text{mol kg}^{-1} \text{yr}^{-1}$). The smaller increase of C_{ANT} in the AAIW layer compared to the SAMW layer (Table 4) agrees with lower ventilation of the AAIW layer south of Tasmania (see section 2) due to the fact that this layer carries recently ventilated waters mixed with older waters ventilated far out the SR03 section. The lack of measurable long-term changes in DIC^{BIO} and DIC^{π} in both AAIW and SAMW layers indicate that circulation and biological processes do not have a large effect on $\frac{\partial DIC}{\partial t}$.

Deep to bottom layers of the section show significant trends for DIC that are not explained by the increase of C_{ANT} . These trends are most likely due to the advection of old and DIC-rich waters. Concretely for deep waters (UCDW and LCDW), the trends could result from an intensification of upwelling at high latitudes being offset by enhanced transport of old and CO_2 -rich waters to replace the upwelled waters, since the increase of DIC follows the upwelling path of the UCDW and LCDW layers (Fig. 4). We separated the UCDW layer into two latitudinal sectors: north and south of the SAF (Fig. 4). The increase of DIC in the UCDW layer north of the SAF is $0.44 \pm 0.04 \mu\text{mol kg}^{-1} \text{yr}^{-1}$ while south of the SAF is smaller at $0.26 \pm 0.04 \mu\text{mol kg}^{-1} \text{yr}^{-1}$ (not shown), consistent with a greater supply of waters from the north at depth. A decrease of O_2 in the UCDW to the north of the SAF occurs mostly in the upper to middle parts of the UCDW layer (Fig. 4), and this is not observed south of the SAF. The decrease of O_2 is also in agreement with the arrival of waters from Indian-Pacific origin since these waters provide the characteristic oxygen minimum zone that defines UCDW (Callahan, 1972; Talley 2013). Another feature that agrees with the hypothesis of upwelling intensification is the shoaling of the ASD following the path of upwelling of the UCDW layer. This feature was also described by Bostock et al. (2013) in an oceanic climatology of Ω_{Ar} and could be due to the naturally lower buffer capacity of the UCDW layer (low value of $TA/DIC \approx 1.043$) with respect to upper layers ($TA/DIC \approx 1.06$ in the AASW layer). However, the greatest shoaling of the ASD in the UCDW layers compared to the AAIW layer (Table 6) is consistent with the upwelling of UCDW, as both water masses have similar TA/DIC ratios ($TA/DIC \approx 1.043$ for the UCDW layer and $TA/DIC \approx 1.042$ for the AAIW layer). Furthermore, the increase of SiO_4 found in deep-bottom layers (Table 4) could also indicate the arrival of old waters to the section that are progressively enriched in SiO_4 (e.g., Callahan, 1972).

Statistically significant decreases in pH_T with time were observed in all water mass layers (Table 4), with the greatest change in surface water masses, coinciding with the greatest DIC changes. The decrease of pH_T in the STCW and SAMW layers is related to the increase in the uptake of C_{ANT} , while for the AASW and AASW_{upw} layers the pH_T change appears to be linked to the upwelling of DIC-rich waters at high latitudes. At deep layers, the tongue of water of $pH_T = 7.9$ off the shelf is reduced in 2011 compared to 1995 (Fig. 2e,f), which is consistent with the advection of DIC-rich waters in the section due to the enhanced upwelling. The different rates of pH_T change in the water masses is in part related to the buffering capacity of the waters. AASW layer has lower temperature than the STCW layer ($\sim 2.3^\circ\text{C}$ for the AASW layer compared to $\sim 11.0^\circ\text{C}$ for the STCW layer, mean values for the period 1995-2011) and lower buffer capacity than the STCW ($TA/DIC \approx 1.058$ for the AASW layer versus $TA/DIC \approx 1.095$ for STCW). For similar increases in DIC (Table 4) the decrease of pH_T in the AASW is expected to be higher than in the STCW layer.

In terms of carbon, previous studies concluded that the intensification of the upwelling (as a consequence of the SAM variability) caused a reduction in the uptake of CO_2 by the Southern Ocean between 1980s and 2000s due to the outgassing of CO_2 near the Antarctic Divergence (Le Quéré et al,


2007; Lovenduski et al., 2008). Landschützer et al. (2015) showed that the efficiency of the Southern Ocean CO₂ sink declined through the 1990's, and the trend reversed from about 2002, although the reversal in the sink efficiency was not zonally uniform. The results from Landschützer et al. (2015) are consistent with a carbon sink influenced by the upwelling of DIC-rich waters at high latitudes and superimposed on this is the near surface response to atmospheric forcing that modifies the sink efficiency and could mask longer term trends in the upwelling of DIC-rich waters at high latitudes. A comparison of our results with those of Landschützer et al. (2015) is problematic as their data is restricted to surface waters and our analysis is on long-term trends in water mass properties below 50m depth. Both data sets do show continued uptake of CO₂ throughout the period of study and indicate the importance of the circulation in influencing the regional carbon sink, which has also been established by recent model results (DeVries et al., 2007).

Our results also agree with the conclusions from different model simulations done by Matear and Lenton (2008), who established that intense wind regimes (associated to a positive phase in the SAM) favour the uptake of C_{ANT} and ventilation of the SAMW and AAIW layers. These authors highlighted the complex response of the uptake of CO₂ by the Southern Ocean due to the diverse forcing acting on upper layers, which can be also seen in our results (e.g., differences in the biogeochemical changes in the AASW and AASW_{upw} layers). Matear and Lenton (2008) also noticed the complex relationship between the upwelling and subduction areas of the Southern Ocean, with the same drivers acting in opposite direction for the changes in non-anthropogenic DIC with respect to the changes in C_{ANT} uptake.

6 Sensitivity of the results to underlying assumptions.

This section considers the sensitivity of assumptions used to calculate temporal changes in C_{ANT}, including errors associated with the assumption of steady state in the oceanic circulation and remineralization processes, and the sensitivity to stoichiometric ratios for the biological processes.

6.1 Comparison of C_{ANT} changes using other methods.

We compared the changes of C_{ANT} obtained in our study with the results from two regression-based methodologies (Table 7); the extended multiple linear regression (eMLR) method (Friis et al., 2005) and the two-regression method (Thacker, 2012). These methods use  eat hydrodynamic sections to quantify the temporal change in C_{ANT}.

The eMLR method (Friis et al., 2005) estimates the change in C_{ANT} between two repeats of a hydrodynamic section by establishing MLRs for each section and relating the observed DIC for each observation to a set of other measured oceanic variables:


$$DIC_{(t)} = a_{0(t)} + a_{1(t)}P_{1(t)} + \dots + a_{n(t)}P_{n(t)} \quad (6)$$

where $a_{x(t)}$ are the coefficients of the fit between DIC and the n observed variables (P_1, \dots, P_n) chosen for the fit, all measured at the time (t) of the survey.

Taking the difference between DIC at two times, t1 and t2, gives an equation for the change in C_{ANT} over the time period between the two hydrographic surveys (ΔC_{ANT}):

$$\Delta C_{ANT} = a_{0(t2)} - a_{0(t1)} + (a_{1(t2)} - a_{0(t1)})P_{1(t2)} + \dots + (a_{n(t2)} - a_{0(t1)})P_{n(t2)} \quad (7)$$

The two-regression method was introduced by Thacker (2012) as an improvement in regression-based methods. The region of study is first divided into sub-regions since the empirical relationships between DIC and other environmental variables vary spatially (Thacker, 2012). MLRs are investigated between DIC and other measured variables (predictors) using a stepwise technique. The procedure is applied for each sub-region using all data from the repeat surveys within the period to be investigated, resulting in an optimal MLR for each sub-region (similar to Eq. 6). A linear regression with time is established for the residuals (observed DIC - predicted DIC) of the regional fits, which directly gives ΔC_{ANT} averaged over the space-time in each sub-region. The purpose of the first MLR is to remove the natural variability of DIC, leaving the anthropogenic signal and noise (random variability) in the residuals and the second MLR is used to separate the anthropogenic signal from the noise.

We applied both methodologies within the different water mass layers separated by γ^n used as sub-regions. The predictor variables of θ , S , σ_θ , nitrate (NO_3), SiO_4 and AOU were used for the MLR procedures. The three methodologies estimate similar rates of increase in C_{ANT} for most water mass layers (Table 7). In the STCW layer, the value of ΔC_{ANT} (eMLR) is higher than our maximum estimate of $\frac{\partial C_{ANT}}{\partial t}$ and the value obtained from the two-regression method. The eMLR method is less suitable for the upper layers of the ocean subject to high seasonal to interannual variability, such as the STCW layer, resulting in large residuals that bias the regression (Friis et al., 2005). For the AAIW layer, the increase of C_{ANT} estimated by the two-regression method is half the increase that is established by our method and the eMLR method. The lower value of the trend estimated by the two-regression method is due to the fact that the two-regression method s stepwise MLR. This means that the two-regression method only considers those predictors that give the best fit while the eMLR method is forced to consider all the predictors in the fit. This is also the cause of the low RMSE obtained with the two-regression method compared to both our trends and those obtained by the eMLR method. For deep to bottom layers, the two-regression method estimates a small increase of C_{ANT} similar to the one found in this study for the AABW layer (Table 7) that can be considered negligible given the resolution of the back-calculation method ($\pm 6 \mu\text{mol kg}^{-1}$). The eMLR method finds increases of C_{ANT} (with relatively high uncertainties) higher than the two-regression method that over the 16-year period also give values of C_{ANT} change lower than the resolution of our back-calculation method (although close to it for the LCDW layer, $\sim 5 \mu\text{mol kg}^{-1}$ for the 16-year period).

6.2 Circulation and biological processes at steady state.

The back-calculation method assumes the circulation of the ocean and the biological processes are in steady state. The contribution of non-linear mixing is unknown and some of the changes in DIC in the water mass layers could be erroneously included in the estimates of C_{ANT} rather than as a non-anthropogenic change in DIC. The non-steady state of the circulation in our analysis is included to some extent through the changes in $CDIS^\pi$ (Eqs. (3, 4), which is solved by the OMP analysis, which is subjected to the limitations of quantifying the mixing mostly through thermohaline changes in the water masses (section A.2 of the Appendix).

For biological processes, remineralization rates are usually considered to be in steady state (Sarmiento et al., 1992). Climate change has been suggested as potentially driving changes in carbon fixation and export that can influence the uptake of CO_2 by the oceans (Falkowski et al., 1998). Pahlow and Riebesell, (2000) first suggested that decadal changes in remineralization rates occurred in the deep waters of the Northern Hemisphere, although this is still a matter of debate (e.g., Li and Peng, 2002; Najjar, 2009).


Metzl et al. (1999) and Shadwick et al. (2015) observed that the uptake of CO₂ over the sub-Antarctic zone (SAZ, between the SAF and the STF) in summer is mostly controlled by biological processes. If a change in remineralization rates has occurred, i.e. the changes in DIC^{BIO} are due to biological effects, a change in nutrient concentrations of the water masses would be expected. The detection of long-term trends of nutrients at upper layers of the ocean can be masked by short time scale physical processes such as changes in the mixed layer depth, mesoscale activity and advection (Sambrotto and Mace, 2000; Rintoul and Trull, 2001; Sallée et al., 2010). We did not find a measurable trend in nutrient concentrations for any of the layers in the period 1995-2011, except for an increase of SiO₄ over the Antarctic Divergence (Table 4) that is most likely due to the upwelling of SiO₄-rich deep waters. We cannot confidently assign the changes of DIC^{BIO} and its impact on $\frac{\partial C_{ANT}}{\partial t}$ in upper layers (Table 5) to any particular process and, instead we provide a range of values for $\frac{\partial C_{ANT}}{\partial t}$ (Table 4). For the scenario of intensification of the Antarctic upwelling, the increase in low-O₂ and DIC-rich waters would increase the content of DIC in subsurface waters, leading (at least for the AASW and AASW_{upw} layers) to values of $\frac{\partial C_{ANT}}{\partial t}$ closer to the lower limit of the range (i.e., $\frac{\partial DIC}{\partial t} \gg \frac{\partial C_{ANT}}{\partial t}$, Table 4).

In deep layers of the section, the increase of DIC is not explained by the long-term change of any of the terms in Eq. (1), which is other implication of considering the circulation in steady state. The differences found in the increase of DIC in the UCDW layer north and south of the SAF (section 4.3, Fig. 4) add consistency to the idea of the advection of older waters to the section. Considering these differences we can assign a change in DIC of at least $\sim 0.20 \pm 0.02 \mu\text{mol kg}^{-1} \text{yr}^{-1}$ (lower rate of increase of DIC found in deep-bottom layers, Table 4) due to the upwelling intensification. Since the AASW and AASW_{upw} layers are the most affected by the upwelling we can correct the values of $\frac{\partial C_{ANT}}{\partial t}$ in these layers for this effect (trends with ** in Table 4).

6.3 Changes in the rates of export of particulate organic carbon silicate from surface layers.

We assume that the export of particulate organic carbon (POC) from upper ocean layers (STCW, AASW and AASW_{upw}) and remineralization in the water column was constant between 1995 and 2011. The high-latitudes are considered important in terms of POC export, mostly because these areas are dominated by large phytoplankton, in particular diatoms (Buesseler, 1998; Sambrotto and Mace, 2000), and rapid carbon export to deep waters from phytoplankton blooms is possible (DiTullio et al., 2000; Lourey and Trull, 2001). The POC exported is remineralized to DIC below the mixed layer (Wassman et al., 1990; Asper and Smith, 1999; Trull et al., 2001a; Fripiat et al., 2015).


Our results show that the increase of DIC in mode and intermediate waters is fully explained by the uptake of atmospheric CO₂, which could indicate that there was no detectable change in the rate of export of POC over the 1995-2011 period. Estimates of POC export in the SAZ (~ 3800 m), the SAF (~ 3100 m) and the PFZ (~ 1500 m) using moored sediment traps near the section (Trull et al., 2001b) were 0.5, 0.8 and 1.0 g C m⁻² yr⁻¹, respectively. If all this POC is fully remineralized in the UCDW layer (with a mean thickness of 2000m), we obtain a range of 0.02 – 0.04 $\mu\text{mol kg}^{-1} \text{yr}^{-1}$ for the maximum

 ease of DIC due to the export of POC. This increase is close to the uncertainty of the total DIC increase estimated for the UCDW layer, which means that in order to generate an increase in DIC similar to that found in the UCDW layer, the rate of POC export should be ~ 10 times higher than the observed rates. This change should be certainly noticeable in $\frac{\partial DIC^{BIO}}{\partial t}$ in surface waters but most probably in deep waters as well, which we do not see.

The observed increase of SiO_4 in deep and bottom layers of the ocean is consistent with the transport of SiO_4 -rich older waters to the section. For UCDW, the increase of SiO_4 north of the SAF is higher than at southern latitudes ($0.31 \pm 0.08 \mu\text{mol kg}^{-1} \text{yr}^{-1}$ respect to $0.19 \pm 0.04 \mu\text{mol kg}^{-1} \text{yr}^{-1}$, not shown). Nelson et al., (1995) observed a lower dissolution rate of diatom dominated SiO_4 exported in high-latitudes regions compared to lower latitudes. Nelson et al. (1995) estimated a mean silica production rate of $0.7 - 1.2 \text{ mol Si m}^{-2} \text{yr}^{-1}$ for regions over diatomaceous sediments and concluded that 15 – 25 % of the silica produced in the upper ocean accumulates in the seabed. Of the silica produced in the mixed layer of the upper ocean layers at least 50% is believed to dissolve in the upper 100 m of the water column (e.g. Nelson et al., 1991; DeMaster et al., 1992). For deep waters, the production rates of Nelson et al. (1995) could result in a mean increase of SiO_4 of $0.08 - 0.14 \mu\text{mol kg}^{-1} \text{yr}^{-1}$ in the water column (~3400 m, mean depth). The maximum value of this increase could explain the trends of SiO_4 found for the AABW layer (Table 4), but 32-48 % of the increase of SiO_4 in deep bottom layers is not explained by the remineralisation of exported silica and is most likely the result of the advection of older SiO_4 -rich waters to the section.

6.4 Stoichiometric ratios for biological processes.


The back-calculation method and the OMP analysis assume constant stoichiometric ratios for remineralization. The theoretical Redfield ratios (Redfield, 1934; 1958) are usually considered as a mean for the whole ocean, although they can vary from the theoretical value due to changes in phytoplankton species composition, the food-web structure and nutrient availability (Martiny et al., 2013).

We carried out a sensitivity analysis on the Redfield ratios following Álvarez et al., (2014), to obtain values of stoichiometric ratios for the section. A battery of OMP analyses  were done with varying values of R_N between 9 and 10 in increments of 0.2, R_P between 120 and 145 in increments of 5, and R_{Si} between 0 and 8 in increments of 2. For each variation in the stoichiometric ratios, an OMP analysis was made for each section in order to determine best-fit R values and if there were differences in time for the stoichiometric ratios along the sections. The smallest residuals (differences between the nutrients measured and the estimated by the OMP analysis) were obtained for $R_N = 9$ and $R_P = 125$. The residuals of SiO_4 did not change significantly for any value of R_{Si} and we consider SiO_4 as a conservative variable. These results indicate $\frac{R_P}{R_N} = 13.8$, in agreement with values obtained for the region ($\frac{R_P}{R_N} \in [8-15]$, Lourey and Trull, 2001).



7 Conclusions.

The results of our analysis south of Tasmania over the 1995-2011 period support a scenario of intensification of upwelling in the vicinity of the Antarctic Divergence due to an increase in the westerly winds at high latitudes most probably linked to the variability of the SAM. The intensification of the upwelling favours the advection of older waters to deep-bottom layers of the section where we found net increase in DIC over the 16-year period. The enhanced upwelling causes the eventual entrainment of low- O_2 and DIC-rich waters into upper layers, explaining the trends of decreasing O_2 and increasing non-anthropogenic DIC found in surface waters close to the Antarctic Divergence. This scenario also implies the intensification of the convergence north of the SAF, implying a more efficient ventilation of the SAMW and AAIW layers and thus an efficient uptake of atmospheric CO_2 by these layers. The enhanced upwelling lowers the uptake of C_{ANT} in the AASW layer but the effect of ventilation more than compensates that of the upwelling allowing the increase in C_{ANT} in this layer.

The atmospheric warming reduces the dissolution of CO₂ in upper layers north of the PF, presenting increases in DIC lower than expected from the atmospheric CO₂ increase.

 results rely on a limited number of sections spread every 3-7 years and can only provide a long term (decadal) average view of changes in water masses. More surface observations and repeat deep ocean sections are needed to help resolve interannual changes in the Southern Ocean carbon sink and to determine the main drivers and feedback to the carbon-climate system. The effort to maintain hydrographic sections with CO₂ system measurements would also benefit from additional direct measurements of more variables of the carbon system, e.g. pH, which has not been measured on the SR03 section.

a availability

 section data are available through the Global Ocean Data Analysis Project (<http://cdiac.ornl.gov/oceans/GLODAPv2>;  et al., 2015; Olsen et al., 2016). The original data for the different cruises were corrected following the QC recommendations in GLODAPv2.

Acknowledgements

The SR03 section was sampled as part of the World Ocean Circulation Experiment/CO₂ Survey (WOCE, <http://woceatlas.ucsd.edu>), and more recently the Global Ocean Ship-Based Hydrographic Investigation Program (GO-SHIPS, <http://www.go-ship.org>). Carbon system parameters contribute to the International Ocean Carbon Coordination Project of the United Nations Intergovernmental Oceanographic Commission (IOCCP, <http://www.ioccp.org>). Support for measurements on the section were provided to S. R. and B. T. by the Antarctic Climate and Ecosystems Cooperative Research Centre (ACE CRC) and the Australian Climate Change Science Program. Logistic support for the section and ship time on the RSV Aurora Australis was provided by the Australian Antarctic Division. The many scientific staff involved in the hydrographic sections and the officers and crew of the ship were critical to obtaining good quality data. We especially want to thank the work by Kate Berry and Mark Pretty for high quality DIC and TA data, and for the hydrochemistry teams and CTD watches of multiple cruises and especially Mark Rosenberg and Rebecca Cowley. The first author of this paper is a postdoctoral fellow supported by the ACE-CRC Project R2.1: Carbon Uptake and Chemical Change.

References.

- Álvarez, M., Brea, S., Mercier, H. and Álvarez-Salgado, X.A.: Mineralization of biogenic materials in the water masses of the South Atlantic Ocean. I: assessment and results of an optimum multiparameter analysis, *Progress in Oceanography*, 123, 1-23, doi: 10.1016/j.pocean.2013.12.007, 2014.
- Anderson, L.A. and Sarmiento, J.L.: Redfield ratios of remineralization determined by nutrient data analysis. *Global Biogeochemical Cycles* 8 (1), 65-80, doi: 10.1029/93GB03318, 1994.
- Aoki, S., Bindoff, N.L. and Church, J.A.: Interdecadal water mass changes in the Southern Ocean between 30°E and 160°E, 32, L07607, doi:10.1029/2004GL022220, 2005.

Aoki, S., et al.: Atlantic–Pacific asymmetry of subsurface temperature change and frontal response of the Antarctic Circumpolar Current for the recent three decades, *J Oceanogr.*, 71, 623–636, doi:10.1007/s10872-015-0284-6, 2015.


Armour, K. and Bitz, C.M.: Observed and projected trends in Antarctic sea ice, *US Clivar Variations Newsletter*, 13, 4, 12-19, 2015.

Asper, V.L. and Smith, W.O.Jr.: Particle fluxes during austral spring and summer in the southern Ross Sea, Antarctica, *J. Geophys. Res.*, 104, C3, 5345-5359, 1999.

Baines, P.G., Edwards, R.J. and Fandry, C.B.: Observations of a new baroclinic current along the western continental slope of Bass Strait, *Aust. J. Mar. Freshwater Res.*, 34, 155–157, 1983.

Bates, N.R., et al.: A time-series view of changing ocean chemistry due to ocean uptake of anthropogenic CO₂ and ocean acidification, *Oceanography* 27, 1, 126–141, <http://dx.doi.org/10.5670/oceanog.2014.16>, 2014.

Belkin, I.M. and Gordon, A.L.: Southern Ocean fronts from the Greenwich meridian to Tasmania, *Journal of Geophysical Research*, 101, C2, 3675-3696, 1996.

Bender, M., et al.: Variability in the /N₂ ratio of southern hemisphere air, 1991-1994: Implications for the carbon cycle, *Global Biogeochemical Cycles*, 10, 1, 9-21, 1996.

Bindoff, N.L. and Church, J.A.: Warming of the Water Column in the Southwest Pacific Ocean, *Nature*, 357, 59-62, 1992.

Bindoff, N.L. and McDougall, T.J.: Diagnosing Climate Change and Ocean Ventilation using Hydrographic Data, *Journal of Physical Oceanography*, 24, 1137-1152, 1994.

Boland, F.M. and Church, J.A.: The East Australian Current 1978, *Deep-Sea Res.*, 28A, 937–957, doi:10.1016/0198-0149(81)90011-X, 1981.

Böning, C.W., Dispert, A., Visbeck, M., Rintoul, S.R. and Schwarzkopf, F.U.: The response of the Antarctic Circumpolar Current to recent climate change, *Nature geoscience*, 1, 864-869, doi:10.1038/ngeo362, 2008.

Bostock, H.C., Mikaloff Fletcher, S.E. and Williams, M.J.M.: Estimating carbonate parameters from hydrographic data for the intermediate and deep waters of the Southern Hemisphere oceans, *Biogeosciences*, 10, 6199–6213, doi:10.5194/bg-10-6199-2013, 2013.

Broecker, W.S.: “NO” a conservative water mass tracer. *Earth and Planetary Science Letters* 23, 8761–8776, 1974.

Buesseler, K.O.: The decoupling of production and particle export in the surface ocean, *Global Biogeochemical Cycles*, 12, 2, 297-310, 1998.


Callahan, J.E.: The structure and circulation of Deep Water in the Antarctic, *Deep-Sea Research*, 19, 563-575, 1972.

Carter, B. R., et al.: Two decades of Pacific anthropogenic carbon storage and ocean acidification along Global Ocean Ship-based Hydrographic Investigations Program sections P16 and P02, *Global Biogeochem. Cycles*, 31, doi:10.1002/2016GB005485, 2017.

Chen, C.-T.A. and Millero, F.J.: Gradual increase of oceanic CO₂, *Nature*, 277, 205–206, 1979.

Chen, C.-T.A., Pytkowicz, M.R. and Olson, E.J.: Evaluation of the calcium problem in the South Pacific, *Geochemical Journal*, 16, 1-10, 1982.

Davis, R.: Intermediate-depth circulation of the Indian and South Pacific oceans measured by autonomous floats, *J. Phys. Oceanogr.*, 35, 683–707, 2005.

 Bacon, G.E.R.: The hydrology of the Southern Ocean, Cambridge University Press, 15, 1-124, 1937.

DeMaster, D.J., et al.: The cycling and accumulation of organic matter and biogenic silica in high-latitude environments: The Ross Sea, *Oceanography*, 5, 146-153, 1992.

DeVries, T., Holzer, M. and Primeau, F.: Recent increase in oceanic carbon uptake driven by weaker upper-ocean overturning, *Nature*, 542, 215-218, doi:10.1038/nature21068, 2017.

Dickson, R.R. and Brown, J.: The production of North Atlantic Deep Water: sources, rates, and pathways, *Journal of Geophysical Research*, 99, C6, 12319-12341, doi:10.1029/94JC00530, 1984.

Dickson, A. G.: Thermodynamics of the dissociation of boric acid in synthetic seawater from 273.15 to 318.15 K, *Deep-Sea Res. I*, 37, 755–766, doi:10.1016/0198-0149(90)90004-F, 1990.

Dickson, A. G. and Millero, F. J.: A comparison of the equilibrium constants for the dissociation of carbonic acid in seawater media, *Deep-Sea Res. I*, 34, 1733–1743, doi:10.1016/0198-0149(87)90021-5, 1987.

Dickson, A.G., Sabine, C.L. and Christian, J.R.: Guide to Best Practices for Ocean CO₂ Measurements, PICES Special Publication 3, 191 pp, 2007.

DiTullio, G.R., et al.: Rapid and early export of *Phaeocystis antarctica* blooms in the Ross Sea, Antarctica, *Nature*, 404, 595-598, 2000.


Doney, S.C., Victoria, J.F., Feely, R.A. and Kleypas, J.A.: Ocean Acidification: The other CO₂ problem, *Annu. Rev. Mar. Sci.*, 1, 169–92, doi:10.1146/annurev.marine.010908.163834, 2009.


Dlugokencky, E.J., Lang, P.M., Mund, J.W., Crotwell, A.M., Crotwell, M.J. and Thoning, K.W.: Atmospheric Carbon Dioxide Dry Air Mole Fractions from the NOAA ESRL Carbon Cycle Cooperative Global Air Sampling Network, 1968-2015, Version: 2016-08-30, ftp://aftp.cmdl.noaa.gov/data/trace_gases/co2/flask/surface/, 2016.

Falkowski, P.G., Barber, R.T. and Smetacek, V.: Biogeochemical Controls and Feedbacks on Ocean Primary Production, *Science*, 281, 5374, 200-206, doi: 10.1126/science.281.5374.200, 1998.

Fay, A. R., McKinley, G.A. and Lovenduski, N.S.: Southern Ocean carbon trends: Sensitivity to methods, *Geophys. Res. Lett.*, 41, 6833–6840, doi:10.1002/2014GL061324, 2014.

Feely, et al.: The impact of anthropogenic CO₂ on the CaCO₃ system in the oceans, *Science*, 305, 362-366, 2004.

Foster, T.D. and Carmack, E.C.: Frontal zone mixing and Antarctic Bottom Water formation in the southern Weddell Sea  *Deep-Sea Research* 23, 301–307, 1976.

Friis, K., Körtzinger, A., J. Pätsch, J., Wallace, D.W.R.: On the temporal increase of anthropogenic CO₂ in the subpolar North Atlantic, *Deep-Sea Research I*, 52, 681–698, doi:10.1016/j.dsr.2004.11.017, 2005. 


Fripiat, F., et al.: Significant mixed layer nitrification in a natural iron-fertilized bloom of the Southern Ocean, *Global*

Biogeochem. Cycles, 29, 1929–1943, doi:10.1002/2014GB005051, 2015.

Fukamachi, Y. et al.: Strong export of Antarctic Bottom Water east of the Kerguelen plateau, *Nature*, 3, 327–331, 2010.


Gordon, A.L. and Tchernia, P.: Waters of the continental margin off Adélie Coast, Antarctica, In: *Antarctic Oceanology II: The Australian–New Zealand Sector*, D.E. Hayes, ed., Antarctic Research Series 19, American Geophysical Union, Washington, DC, 59–69, 1972.

Gruber, N.: Anthropogenic CO₂ in the Atlantic Ocean, *Global Biogeochemical Cycles*, 12, 1, 165–191, 1998.

ber, et al.: Oceanic sources, sinks, and transport of atmospheric CO₂. *Global Biogeochemical Cycles*, 23, GB1005, doi:10.1029/2008GB003349, 2009.

Hanawa, K. and Talley, L.D.: Mode waters, In: Siedler, G., Church, J., Gould, J. (Eds.), *Ocean Circulation and Climate*, International Geophysics Series, Academic Press, New York, 373–386, 2001.

Hauri, C., et al.: Two decades of inorganic carbon dynamics along the West Antarctic Peninsula, *Biogeosciences*, 12, 6761–6779, doi:10.5194/bg-12-6761-2015, 2015.

m, K. P., Bindoff, N.L., and Church, J.A.: Observed decreases in oxygen content of the global ocean, *Geophys. Res. Lett.*, 38, L23602, doi:10.1029/2011GL049513, 2011.

Herraz-Borreguero, L and Rintoul, S.R.: Regional circulation and its impact on upper ocean variability south of Tasmania, *Deep-Sea Research II*, 58, 2071–2081, doi:10.1016/j.dsr2.2011.05.022, 2011.

Hill, K.L., Rintoul, S.R., Ridgway, K.R. and Oke, P.R.: Decadal changes in the South Pacific western boundary current system revealed in observations and ocean state estimates, *J. Geophys. Res.*, 116, C01009, doi:10.1029/2009JC005926, 2001.

Hood, E. M., Sabine, C. L. and Sloyan, B. M.: *The GO-SHIP Repeat Hydrography Manual: a Collection of Expert Reports*

and Guidelines, IOCCP Report Number 14, OCPO Publication Series Number 134, <http://www.go-ship.org/HydroMan.html>, 2010.

Ikegami, H. and Kanamori, S.: Calcium-Alkalinity-Nitrate Relationship in the North Pacific and the Japan Sea, *Journal of the Oceanographical Society of Japan*, 39, 9–14, 1983.

Iudicone, D., Speich, S., Madec, G. and Blanke, B.: The Global Conveyor Belt from a Southern Ocean perspective, 38, 1401–1425, doi:10.1175/2007JPO3525.1, 2008.


Jackett, D.R. and McDougall, T.J.: A Neutral Density Variable for the World's Oceans, *Journal of Physical Oceanography*, 27, 237–263, 1997.

Jacobs, S. S.: On the nature and significance of the Antarctic Slope Front, *Mar. Chem.*, 35, 9 –24, 1991.


Jacobs, S.: Observations of change in the Southern Ocean, *Phil. Trans. R. Soc. A*, 364, 1657–1681, doi:10.1098/rsta.2006.1794, 2006.

Johnson, G.C.: Quantifying Antarctic Bottom Water and North Atlantic Deep Water volumes, *J. Geophys. Res.*, 113, C05027, doi:10.1029/2007JC004477, 2008.

Joyce, T. and Corry, C., 1994: Requirements for WOCE Hydrographic Programme Data Reporting, WHPO Publication 90-1 Revision 2, WOCE Report 67/91, Woods Hole, Mass., USA, 1994.

 R.M., et. al: Global Ocean Data Analysis Project, Version 2 (GLODAPv2), ORNL/CDIAC-162, NDP093. Carbon Dioxide Information Analysis Center, Oak Ridge National Laboratory, US Department of Energy, Oak Ridge, Tennessee. doi: 10.3334/CDIAC/OTG.NDP093_GLODAPv2, 2015.

Khatiwala, S., Primeau, F. and Hall, T.: Reconstruction of the history of anthropogenic CO₂ concentrations in the ocean, *Nature*, 462, 346-350, doi:10.1038/nature08526, 2009.

Kouketsu, S., Murata, A.M.: Detecting decadal scale increases in anthropogenic CO₂ in the ocean, *Geophys. Res. Lett.*, 41, 4594–4600, doi:10.1002/2014GL060516, 2014. 

Landschützer, P., et al.: The reinvigoration of the Southern Ocean carbon sink, *Science*, 349, 1221–1224, doi:10.1126/science.aab2620, 2015.

Lauvset, S.K., Gruber, N., Landschützer, P., Olsen, A. and Tjiputra, J.: Trends and drivers in global surface ocean pH over

the past 3 decades, *Biogeosciences*, 12, 1285–1298, doi:10.5194/bg-12-1285-2015, 2015.

Lenton, A. and Matear, R.J.: Role of the Southern Annular Mode (SAM) in Southern Ocean CO₂ uptake, *Global Biogeochem. Cycles*, 21, GB2016, doi:10.1029/2006GB002714, 2007.

Lenton, A., et al.: *Global Biogeochemical Cycles*, 26, GB2021, doi:10.1029/2011GB004095, 2012.

Lenton, A., et al.: Sea–air CO₂ fluxes in the Southern Ocean for the period 1990–2009, *Biogeosciences*, 10, 4037–4054, doi:10.5194/bg-10-4037-2013, 2013.

Le Quéré, C., et al.: Saturation of the Southern Ocean CO₂ Sink Due to Recent Climate Change, *Science* 316, 1735–1738, doi: 10.1126/science.1136188, 2007.

Le Quéré, C., et al.: Global carbon budget 2014, *Earth Syst. Sci. Data*, 7, 47–85, doi:10.5194/essd-7-47-2015, 2015.

Lewis, E. and Wallace, D.W.R.: Program Developed for CO₂ System Calculations. ORNL/CDIAC-105. Carbon Dioxide Information Analysis Center, Oak Ridge National Laboratory, U.S. Department of Energy, Oak Ridge, Tennessee, 1998.

Lourey, K.J. and Trull, T.W.: Seasonal nutrient depletion and carbon export in the Subantarctic and Polar Frontal Zones of the Southern Ocean south of Australia, *J. Geophys. Res.*, 106, C12, 31,463–31,487, 2001.

Lovenduski, N.S., Gruber, N. and Doney, S.C.: Towards a mechanistic understanding of the decadal trends in the Southern Ocean carbon sink, *Global Biogeochemical Cycles*, 22, GB3016, doi:10.1029/2007GB003139, 2008.

Lumpkin, R. and Speer, K.: Global Ocean Meridional Overturning, *Journal of Physical Oceanography*, 37, 2550–2562, doi:10.1175/JPO3130.1, 2007.

Mantyla, A.W. and Reid, J.L.: On the origins of deep and bottom waters of the Indian Ocean, *Journal of Geophysical Research*, 100, C2, 2417–2439, 1995.

Marshall, G.J.: Analysis of recent circulation and thermal advection change in the northern Antarctic Peninsula, *Int. J. Climatol.*, 22, 1557–1567, doi:10.1002/joc.814, 2002.

Marshall, G.J.: Trends in the Southern Annular Mode from observations and reanalyses, *Journal of Climate*, 16, 4134-4143, 2003.

Marsland, S. J., Bindoff, N.L., Williams, G.D. and Budd, W.F.: Modeling water mass formation in the Mertz Glacier Polynya and Adélie Depression, East Antarctica, *J. Geophys. Res.*, 109, C11003, doi:10.1029/2004JC002441, 2004.

Matear, R.J., Hirst, A.C. and McNeil, B.I.: Changes in dissolved oxygen in the Southern Ocean with climate change, *Geochem. Geophys. Geosyst.*, 1, 2000GC000086, ISSN: 1525-2027, 2000.

Matear, R. and Lenton, A.: Impact of historical climate change on the Southern Ocean carbon cycle, *Journal of Climate*, 21, 5820-5834, doi:10.1175/2008JCLI2194.1, 2008.

McCartney, M.S.: The subtropical recirculation of mode waters. *J. Mar. Res.*, 40 (Suppl.), 427-464, 1977.

McDougall, T.J.: Neutral surfaces in the ocean: implications for modelling, *Geophysical Research Letters*, 14, 8, 97-800, 1987.

McNeil, B.I., Tilbrook, B. and Matear, R.J.: Accumulation and uptake of anthropogenic CO₂ in the Southern Ocean, south of Australia between 1968 and 1996, *Journal of Geophysical Research*, 106, C12, 31431-31445, 2001.

Mehrbach, C., Culberson, C.H., Hawley, J.E. and Pytkowicz, R.M.: Measurement of the apparent dissociation constants of carbonic acid in seawater at atmospheric pressure, *Limnol. Oceanogr.*, 18, 897-907, doi:10.4319/lm.1973.18.6.0897, 1973.

Metzl, N., Tilbrook, B. and Poisson, A.: The annual fCO₂ cycle and the air-sea CO₂ flux in the sub-Antarctic Ocean, *Tellus*, 51B, 849-861, 1999.

Moore, J.K. and Abbott, M.R.: Phytoplankton chlorophyll distributions and primary production in the Southern Ocean, *J. Geophys. Res.*, 105, C12, 28709-28722, 2000.

Moore, J.K., Abbott, M.R. and Richman, J.R.: Location and dynamics of the Antarctic Polar Front from satellite sea surface temperature data, *J. Geophys. Res.*, 104, 3059-3073, 1999.


Morrow, R., Donguy, J.-R., Chaigneau, A. and Rintoul, S.R.: Cold-core anomalies at the subantarctic front, south of Tasmania, *Deep-Sea Res. I*, 51, 1417-1440, 2004.

Murata, A., Kumamoto, Y., Watanabe, S. and Fukasawa, M.: Decadal increases of anthropogenic CO₂ in the South Pacific subtropical ocean along 32°S, *J. Geophys. Res.*, 112, C05033, doi:10.1029/2005JC003405, 2007.

Najjar, R.: The dark side of marine carbon, *Nature geoscience*, 2, 603-604, doi: 10.1038/NGEO812, 2009.

Nelson, D.M., Ahern, J.A. and Herlihy, L.J.: Cycling of biogenic silica within the upper water column of the Ross Sea, *Mar. Chem*, 35, 461-476, 1991.

Nelson, D.M., et al.: Production and dissolution of biogenic silica in the ocean: Revised global estimates, comparison with regional data and relationship to biogenic sedimentation, *Global Biogeochemical Cycle*, 9, 3, 359-372, 1995.

 en, A., et al.: The Global Ocean Data Analysis Project version 2 (GLODAPv2) – an internally consistent data product for the world ocean, *Earth Syst. Sci. Data*, 8, 297–323, 2016, doi:10.5194/essd-8-297-2016, 2016.

Orr, J.C., et al.: Anthropogenic ocean acidification over the twenty-first century and its impact on calcifying organisms, *Nature*, 437, 681–686, doi:10.1038/nature04095, 2005.

Orsi, A.H., Whitworth III, T. and Nowlin, W.D.: On the meridional extent and fronts of the Antarctic Circumpolar Current. *Deep Sea Research I*, 42, 5, 641–673, 1995.

Pahlow, M. and Riebesell, U.: Temporal trends in deep ocean Redfield ratios, *Science*, 287, 831–833, 2000.

Pardo, P.C., Vázquez-Rodríguez, M., Pérez, F.F. and Ríos, A.F.: CO₂ air-sea disequilibrium and preformed alkalinity in the Pacific and Indian Oceans calculated from subsurface layer data, *Journal of Marine Systems* 84, 67–77, doi:10.1016/j.jmarsys.2010.08.006, 2011.

Pardo, P.C., Pérez, F.F., Khatiwala, S. and Ríos, A.F.: Anthropogenic CO₂ estimates in the Southern Ocean: Storage partitioning in the different water masses, *Progress in Oceanography*, 120, 230–242, doi:10.1016/j.pocean.2013.09.005, 2014.

Peña-Molino, B., Rintoul, S.R. and Mazloff, M.R.: Barotropic and baroclinic contributions to along-stream and across-stream transport in the Antarctic Circumpolar Current, *J. Geophys. Res. Oceans*, 119, 8011–8028, doi:10.1002/2014JC010020, 2014.

Purkey, S.G. and Johnson, G.C.: Global Contraction of Antarctic Bottom Water between the 1980s and 2000s, *Journal of Climate*, 25, 5830–5844, doi:10.1175/JCLI-D-11-00612.1, 2012.

Redfield, A.: On the proportions of organic derivatives in sea water and their relation to the composition of plankton, In Daniel, R.J. (ed James Johnstone Memorial Volume). University Press of Liverpool, 177–192, 1934.

Redfield, A.: The biological control of chemical factors in the environment, *Am. Sci.*, 46, 205–221, 1958.

Ridgway, K.R.: Seasonal circulation around Tasmania: An interface between eastern and western boundary dynamics, *J. Geophys. Res.*, 112, C10016, doi:10.1029/2006JC003898, 2007.

Rintoul, S.R.: On the origin and influence of Adelie Land Bottom Water, *Ocean, Ice, and Atmosphere: Interactions at the Antarctic continental margin Antarctic Research Series*, 75, 151–171, 1998.

Rintoul, S.R. and Bullister, J.L.: A late winter hydrographic section from Tasmania to Antarctica, *Deep-Sea Research I*, 46, 1417–1454, 1999.

Rintoul, S.R. and England, M.H.: Ekman Transport Dominates Local Air–Sea Fluxes in Driving Variability of Subantarctic Mode Water, *Journal of Physical Oceanography*, 32, 1308–1321, 2002.

Rintoul, S.R. and Sokolov, S.: Baroclinic transport variability of the Antarctic Circumpolar Current south of Australia (WOCE repeat section SR3), *J. Geophys. Res.*, 106, C2, 2815–2832, 2001.

Rintoul, S.R. and Trull, T.W.: Seasonal evolution of the mixed layer in the Subantarctic Zone south of Australia, *Journal of Geophysical Research*, 106, C12, 31447–31462, 2001.

Rintoul, S.R., Donguy, J.R. and Roemmich, D.H.: Seasonal evolution of upper ocean thermal structure between Tasmania and Antarctica, *Deep-Sea Research I*, 44, 1, 1185–1202, 1997.

Sabine, C.L., et al.: The Oceanic Sink for Anthropogenic CO₂, *Science*, 305, 5682, 367–371, 2004.

Sabine, C.L., et al.: Decadal changes in Pacific carbon, *J. Geophys. Res.*, 113, C07021, doi:10.1029/2007JC004577, 2008.

Sallée, J.B., Matear, R.J., Rintoul, S.R. and Lenton, A.: Localized subduction of anthropogenic carbon dioxide in the Southern Hemisphere oceans, *Nature*, 5, 579-584, doi: 10.1038/NGEO1523, 2012.

Sallée, J.B., Speer, K. and Morrow, R.: Response of the Antarctic Circumpolar Current to Atmospheric Variability, *Journal of Climate*, 21, 3020-3039, doi:10.1175/2007JCLI1702.1, 2008.

Sallée, L.B., Speer, K.G. and Rintoul, S.R.: Zonally asymmetric response of the Southern Ocean mixed-layer depth to the Southern Annular Mode, 3, 273-279, 2010.

Sallée, J.-B., Wienders, N., Speer, K. and Morow, R.: Formation of subantarctic mode water in the southeastern Indian Ocean, *Ocean Dynamics*, 56, 525-542, doi:10.1007/s10236-005-0054-x, 2006.

Sambrotto, R.N. and Mace, B.J.: Coupling of biological and physical regimes across the Antarctic Polar Front as reflected by nitrogen production and recycling, *Deep-Sea Res. II*, 47, 3339-3367, 2000.

Sarmiento, J.L. and Sundquist, E.T.: Revised budget for the oceanic uptake of anthropogenic carbon dioxide, *Nature*, 356, 589-593, 1992.

Sarmiento, J.L., Gruber, N., Brzezinski, M.A. and Dunne, J.P.: High-latitude controls of thermocline nutrients and low latitude biological productivity. *Nature*, 427, 56–60, 2004.

Sarmiento, J.L., Hughes, T.M.C., Stouffer, R.J. and Manabe, S.: Simulated response of the ocean carbon cycle to anthropogenic climate warming, *Nature*, 393, 245-249, 1998.

Sedwick, P.N., et al.: Limitation of algal growth by iron deficiency in the Australian Subantarctic region, *Geophys. Res. Lett.*, 26, 18, 2865-2868, 1999.

Shadwick, E. H., et al.: Seasonality of biological and physical controls on surface ocean CO₂ from hourly observations at the Southern Ocean Time Series site south of Australia, *Global Biogeochem. Cycles*, 29, doi:10.1002/2014GB004906, 2015.

Sloyan, B.M. and Rintoul, S.R.: The Southern Ocean Limb of the Global Deep Overturning Circulation, *Journal of Physical Oceanography*, 31, 143-173, 2001.

Sloyan, B.M., Ridgway, K. and Cowley, R.: The East Australian Current and Property Transport at 27°S from 2012 to 2013, *Journal of Physical Oceanography*, 46, 993-1008, DOI: 10.1175/JPO-D-15-0052.1, 2016.

Sokolov, S. and Rintoul, S.R.: Structure of Southern Ocean fronts at 140°E, *Journal of Marine Systems*, 37, 151-184, 2002.

Sokolov, S. and Rintoul, S.R.: Multiple jets of the Antarctic Circumpolar Current South of Australia, *Journal of Phys. Ocean.* 37, 1394-1412, doi: 10.1175/JPO3111.1, 2007.

Sokolov, S. and Rintoul, S.R.: Circumpolar structure and distribution of the Antarctic Circumpolar Current fronts: 1. Mean circumpolar paths, *Journal of Geophysical Research*, 114, C11018, doi:10.1029/2008JC005108, 2009.

Speer, K., Rintoul, S.R. and Sloyan, B.: The Diabatic Deacon Cell, *Journal of Physical Oceanography*, 30, 3212-3222, 2000.

Speich, S., et al.: Tasman leakage: A new route in the global ocean conveyor belt, *Geophysical Research Letters*, 29, 10, 1416, 10.1029/2001GL014586, 2002.

Talley, L.D.: Closure of the global overturning circulation through the Indian Pacific, and Southern Oceans: Schematics and transports, *Oceanography* 26, 1, 80-97, <http://dx.doi.org/10.5670/oceanog.2013.07>, 2013.

Thacker, W.C.: Regression-based estimates of the rate of accumulation of anthropogenic CO₂ in the ocean: A fresh look, *Marine Chemistry*, 132–133, 44–55, doi:10.1016/j.marchem.2012.02.004, 2012.

Thompson, D.W.J. and Solomon, S.: Interpretation of Recent Southern Hemisphere Climate Change, *Science*, 296, 895-899, doi:10.1126/science.1069270, 2002.

Tomczak, M.: A multi-parameter extension of temperature/salinity diagram techniques for the analysis of non-isopycnal mixing, *Progress in Oceanography*, 10, 147–171, 1981.

Tréguer, P., et al.: The Silica Balance in the World Ocean: A Reestimate, *Science*, 268, 5209, 375-379, doi: 10.1126/science.268.5209.375, 1995.


Tréguer, P.J.: The Southern Ocean silica cycle  *Comptes Rendus* Geoscience, 346, 279–286, 10.1016/j.crte.2014.07.003, 2014.

Trull, T., Rintoul, S.R., Hadfield, M. and Abraham, E.R.: Circulation and seasonal evolution of polar waters south of Australia: Implications for iron fertilization of the Southern Ocean, *Deep-Sea Res. II*, 2439-2466, 2001a.

Trull, T.W., et al.: Moored sediment trap measurements of carbon export in the Subantarctic and Polar Frontal Zones of the Southern Ocean, south of Australia, *J. Geophys. Res.*, 106, C12, 489-31,509, 2001b.


Uppstrom, L. R.: The boron/chlorinity ratio of deep-sea water from the Pacific Ocean, *Deep-Sea Research*, 21, 161-162, 1974

van Heuven, S., Pierrot, D., Rae, J.W.B., Lewis, E. and Wallace, D.W.R.: MATLAB Program Developed for CO₂ System Calculations, 2011.

 Heuven, S., Hoppema, M., Jones, E.M., de Baar, H.J.W.: Rapid invasion of anthropogenic CO₂ into the deep circulation of the Weddell Gyre. *Phil. Trans. R. Soc. A* 372: 20130056. <http://dx.doi.org/10.1098/rsta.2013.0056>, 2014.

van Wijk, E. M. and Rintoul, S.R.: Freshening drives contraction of Antarctic Bottom Water in the Australian Antarctic Basin, *Geophys. Res. Lett.*, 41, 1657–1664, doi:10.1002/2013GL058921, 2014.

Vázquez-Rodríguez, M., Padín, X.A., Pardo, P.C., Ríos, A.F. and Pérez, F.F.: The subsurface layer reference to calculate preformed alkalinity and air-sea CO₂ disequilibrium in the Atlantic Ocean. *Journal of Marine Systems* 94, 52–63, doi:10.1016/j.jmarsys.2011.10.008, 2012.

Verdy, A., Dutkiewicz, S., Follows, M.J., Marshall, J. and Czaja, A.: Carbon dioxide and oxygen fluxes in the Southern Ocean:  Mechanisms of Interannual variability, *Global Biogeochemical Cycles*, 21, GB2020, doi:10.1029/2006GB002916, 2007.

Wang, X., Matear, R.J. and Trull, T.W.: Nutrient utilization ratios in the Polar Frontal Zone in the Australian sector of the Southern Ocean: A model, *Global Biogeochem. Cycles*, 17,1, 1009, doi:10.1029/2002GB001938, 2003.

Wassmann, P., Vernet, M., Mitchell, B.G. and Rey, F.: Mass sedimentation of *Phaeocystis pouchetii* in the Barents Sea, Marine Ecology Progress Series, 66, 183-195, 1990.

Waters, J.F., Millero, F.J. and Sabine, C.L.: Changes in South Pacific anthropogenic carbon, Global Biogeochem. Cycles, 25, GB4011, doi:10.1029/2010GB003988, 2011.

Weiss, R.: Carbon dioxide in water and seawater: the solubility of a non-ideal gas, Mar. Chem., 2, 203–215, doi:10.1016/0304-4203(74)90015-2, 1974.


Whitworth III, T. and Nowlin Jr., W.D.: Water masses and currents of the Southern Ocean at the Greenwich meridian, Journal of Geophysical Research, 92, C6, 6462-6476, 1987.

Williams, N.L., et al.: Quantifying anthropogenic carbon inventory changes in the Pacific sector of the Southern Ocean, Marine Chemistry, 174, 147–160, doi: /10.1016/j.marchem.2015.06.015, 2015

Wong, A.P.S., Bindoff, N.L. and Church, J.A.: Large-scale freshening of intermediate waters in the Pacific and Indian oceans, Nature, 400, 440-443, 1999.

Xue, L., Gao, L., Cai, W.-J., Yu, w. and Wei, M.: Response of sea surface fugacity of CO₂ to the SAM shift south of Tasmania: Regional differences, Geophys. Res. Lett., 42, 3973–3979, doi:10.1002/2015GL063926, 2015.

Zickfeld, K., et al.: Response of the global carbon cycle to human-induced changes in Southern Hemisphere winds, Geophysical Research Letters, 34, L12712, doi:10.1029/2006GL028797, 2007.

 Zickfeld, K., Fyfe, J.C., Eby, M. and Weaver, A.J.: Comment on "Saturation of the Southern Ocean CO₂ Sink Due to Recent Climate Change", Science 319, 5863, 570b, doi: 10.1126/science.1146886, 2008.

B Figures

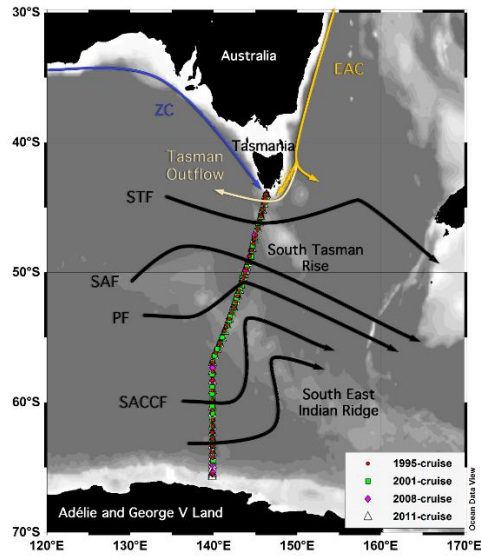


Fig. 1. Transects of the 4 summer repeats of the G0-SHIP hydrodynamic line SR03 in the Southern Ocean south of Tasmania for the period 1995 – 2011 and main hydrography features of the region. ZC = Zeehan Current. EAC = East Australian Current. Black arrows indicate the flow of the Antarctic Circumpolar Current (ACC), with STF = Subtropical Front; SAF = Sub-Antarctic Front, PF = Polar Front and SACCF = Southern ACC Front.

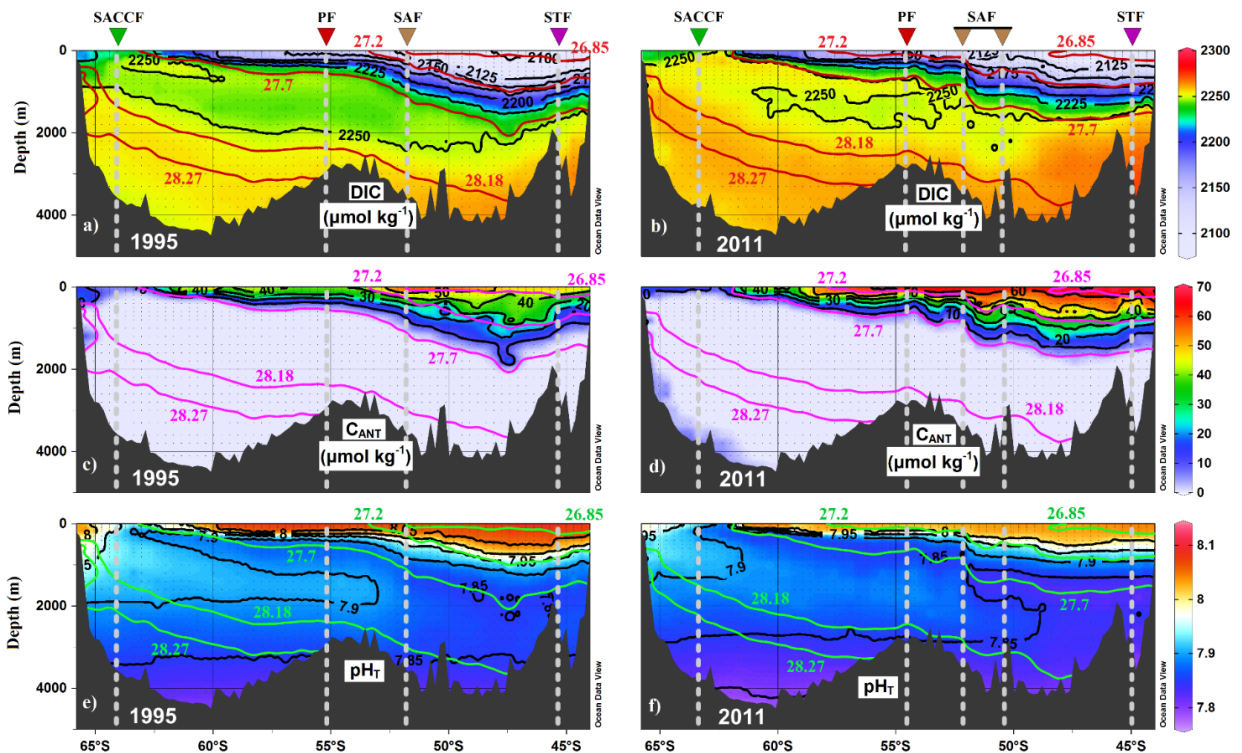


Fig. 2. Distribution of DIC (a and b), C_{ANT} (c and d) and pH_T (e and f) in the SR03 section south of Tasmania for the years 1995 (a, c, e) and 2011 (b, d, f). Red lines in plots (a) and (b), pink lines in plots (c) and (d) and green lines in plots (e) and (f) indicate the neutral surfaces that define the different water masses (σ_θ). The position of the fronts (coloured triangles and grey dotted lines) in each of the cruises is also shown.

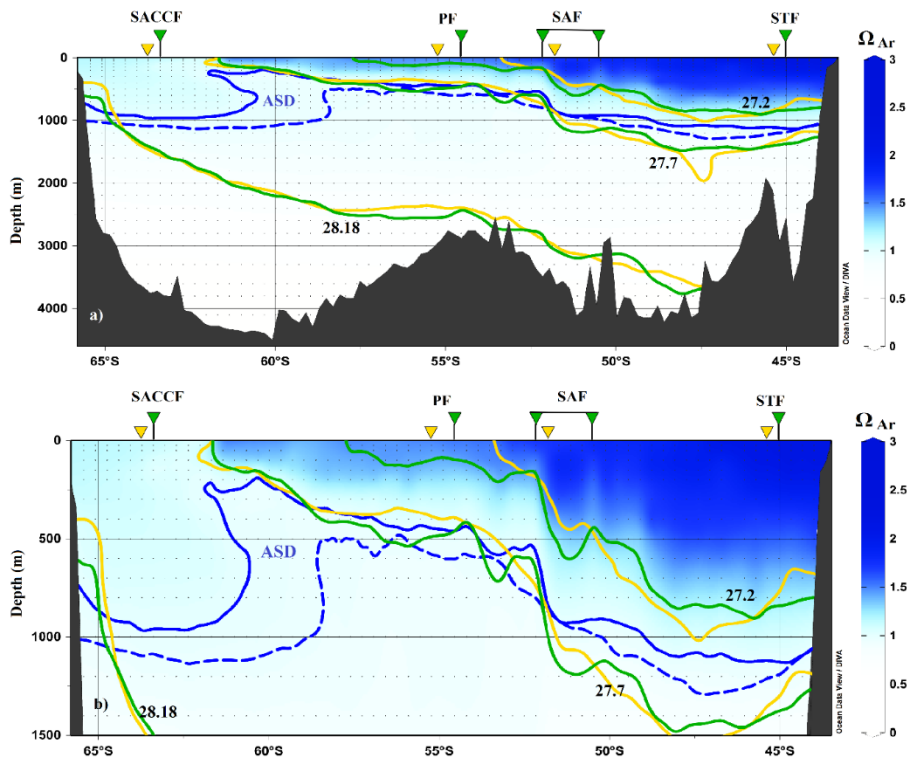


Fig. 3. Aragonite Saturation Depth (ASD, $\Omega_{Ar} = 1$) for the 1995 and 2011 cruises. (a) Distribution of ASD (blue dotted and solid lines) and γ^n (green and yellow lines) in latitude in the SR03 section. (b) section zoomed for the first 1500 m of the water column. The position of the fronts (triangles) in 1995 (yellow) and 2011 (green) is also shown. The blue palette in the background indicates the distribution of Ω_{Ar} for the 2011-cruise.

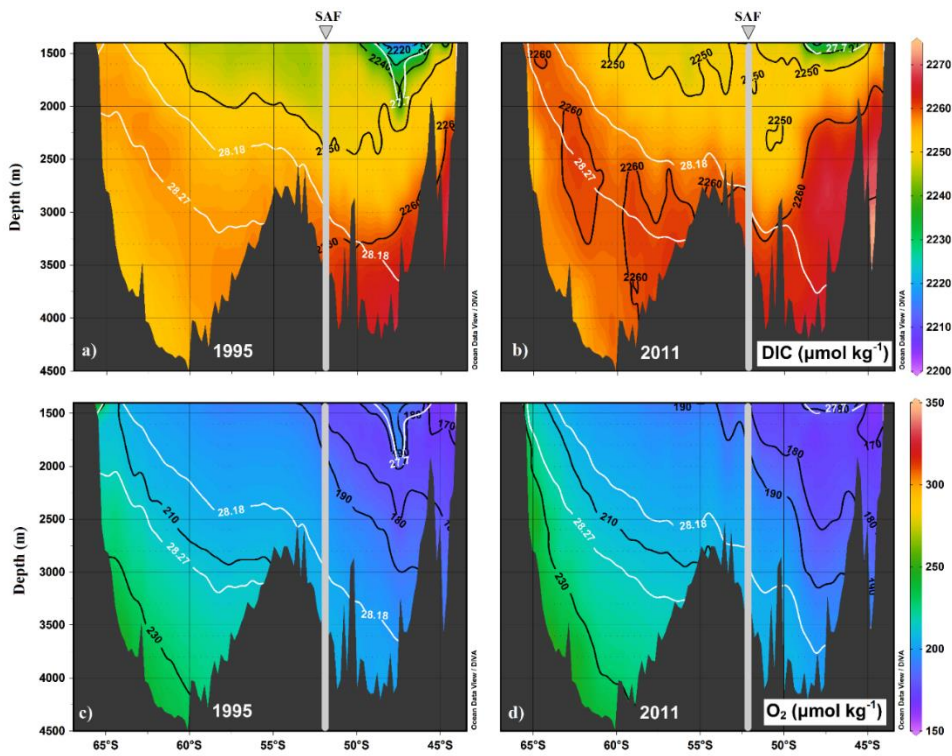




Fig. 4. Distribution of (a and b) dissolved inorganic carbon (DIC) and (c and d) dissolved oxygen (O_2) in the 1995 and 2011 cruises for deep-bottom layers of the section. The location of the Sub-Antarctic Front (SAF) is also shown as well as the neutral surfaces (γ^n , white lines) limiting the UCDW, LCDW and AABW layers.

C Tables



EXPOCODE	Dates	REF.
09AR19941213	20/12/1994 - 1/02/1995	1995
09AR20011029	29/10/2001 - 11/12/2001	2001
09AR20080322	23/03/2008 - 15/04/2008	2008
09AR20110124	4/01/2011 - 31/01/2011	2011

Table 1. Repeats of the GO-SHIP SR03 line on board the Aurora Australis from 1995 to 2011 with the expocode from GLODAPv2 database.

Layer	Definition	Complete Name	Reference
STCW	$\gamma^n < 26.85$ & $S \geq 34.3$	Subtropical Central Water	Rintoul (1998)
AASW	$\gamma^n < 27.7$ & $S < 34.3$	Antarctic Surface Water	Rintoul (1998); Williams et al. (2015)
AASW _{upper}	$\gamma^n \geq 27.7$ & depth ≤ 300 m	Antarctic Surface Water	-----
SAMW	$26.85 \leq \gamma^n < 27.2$ & $S \geq 34.3$	Sub-Antarctic Mode Water	Rintoul (1998); Rintoul and Bullister (1999)
AAIW	$27.2 \leq \gamma^n < 27.7$ & $S \geq 34.3$	Antarctic Intermediate Water	Rintoul and Bullister (1999)
UCDW	$27.7 \leq \gamma^n < 28.18$ & depth > 300 m	Upper Circumpolar Deep water	Williams et al. (2015)
LCDW	$28.18 \leq \gamma^n < 28.25$	Lower Circumpolar Deep Water	Lacarra et al. (2011); Williams et al. (2015)
AABW	$\gamma^n \geq 28.25$	Antarctic Bottom Water	Rintoul and Bullister (1999); Williams et al. (2015)

Table 2. Definition of the water mass layers between neutral surfaces (γ^n) and  references used to accordingly decide the limits of the layers. We also consider limits in salinity, depth and position of the ACC fronts (see Table 3) to differentiate better some of the layers .

Cruise	STF	SAF	PF	SACCF
1995	~45.4°S	~51.8°S	~55.2°S	~63.8°S
2001	~46.4°S	~50.1°S	~54.5°S	~63.7°S
2008	~46.4°S	~52.2°S	~54.6°S	~63.5°S
2011	~45°S	~52.16-50.5°S *	~54.5°S	~63.4°S

Table 3. Location of the ACC fronts south of Tasmania for each of the cruises following the definitions of Sokolov and  Rintoul (2002) for hydrographic data. * The range in the location of the SAF for the 2011-cruise could be related to a  rsification of the PF or SAF into different jets (Sokolov and Rintoul, 2009) but also to crossing the meander of the front twice.

Layer	$\partial \text{DIC} / \partial t$ ($\mu\text{mol kg}^{-1} \text{yr}^{-1}$) 1995-2011	$\partial C_{\text{ANT}} / \partial t$ ($\mu\text{mol kg}^{-1} \text{yr}^{-1}$) 1995-2011	$\partial \text{SiO}_4 / \partial t$ ($\mu\text{mol kg}^{-1} \text{yr}^{-1}$) 1995-2011	$\partial \text{pH}_T / \partial t$ (yr^{-1}) 1995-2011	$\partial \Omega_{\text{Ar}} / \partial t$ (yr^{-1}) 1995-2011	% $\partial \Omega_{\text{Ar}} / \partial t$ (% yr^{-1}) 1995-2011
STCW	0.86 ± 0.07 , RMSE=7	$[0.71 \pm 0.08 - 0.93 \pm 0.08]$	-----	-0.0027 ± 0.0001 , RMSE=0.01	-0.009 ± 0.001 , RMSE=0.15	-0.42 ± 0.17
AASW	0.85 ± 0.14 , RMSE=21	$[0.35 \pm 0.14 - 0.85 \pm 0.21]$ * $[0.35 \pm 0.14 - 0.65 \pm 0.21]$	-----	-0.0035 ± 0.0002 , RMSE=0.03	-0.009 ± 0.001 , RMSE=0.14	-0.61 ± 0.19
AASW _{upw}	0.61 ± 0.10 , RMSE=9	$[0 - 0.41 \pm 0.16]$ * $[0 - 0.21 \pm 0.16]$	0.36 ± 0.06 , RMSE=6	-0.0015 ± 0.0004 RMSE=0.04	-----	-----
SAMW	1.10 ± 0.14 , RMSE=16	0.92 ± 0.09 , RMSE=10	-----	-0.0031 ± 0.0003 RMSE=0.03	-0.011 ± 0.001 , RMSE=0.17	-0.67 ± 0.20
AAIW	0.40 ± 0.15 , RMSE=24	0.42 ± 0.06 , RMSE=10	-----	-0.0017 ± 0.0002 RMSE=0.03	-----	-----
UCDW	0.29 ± 0.02 , RMSE=5	-----	0.22 ± 0.04 , RMSE=12	-0.0012 ± 0.0001 RMSE=0.03	-----	-----
LCDW	0.20 ± 0.02 , RMSE=4	-----	0.27 ± 0.02 , RMSE=4	-0.0012 ± 0.0002 RMSE=0.03	-----	-----
AABW	0.24 ± 0.02 , RMSE=2	** 0.07 ± 0.01 , RMSE=2	0.15 ± 0.05 , RMSE=11	-----	-----	-----

Table 4. Trends in the water mass layers for the period 1995-2011 of dissolved inorganic carbon ($\partial \text{DIC} / \partial t$), anthropogenic carbon ($\partial C_{\text{ANT}} / \partial t$), silicate ($\partial \text{SiO}_4 / \partial t$) total pH ($\partial \text{pH}_T / \partial t$), aragonite saturation ($\partial \Omega_{\text{Ar}} / \partial t$) and % of change in the aragonite saturation (% $\partial \Omega_{\text{Ar}} / \partial t$). RMSE = root mean square error. * Trends in C_{ANT} for the AASW and AASW_{upw} layers considering an approximate value for the increase in DIC due to the advection of old deep waters to the section (see section 4.4.1 in the text). ** The value of $\frac{\partial C_{\text{ANT}}}{\partial t}$ in the AABW layer is considered negligible because it falls below the accuracy of the back-calculation method.

Layer	$\partial C_{\text{ANT}_{\text{BC}}} / \partial t$ ($\mu\text{mol kg}^{-1} \text{yr}^{-1}$) 1995-2011	$\partial \text{DIC}^{\text{BIO}} / \partial t$ ($\mu\text{mol kg}^{-1} \text{yr}^{-1}$) 1995-2011	$\partial \text{DIC}^{\pi} / \partial t$ ($\mu\text{mol kg}^{-1} \text{yr}^{-1}$) 1995-2011
STCW	1.05 ± 0.05 , RMSE=5	0.22 ± 0.08 , RMSE=8	-0.34 ± 0.06 , RMSE=6
AASW	0.71 ± 0.06 , RMSE=9	0.50 ± 0.16 , RMSE=23	-0.36 ± 0.13 , RMSE=17
AASW _{upw}	-----	0.41 ± 0.16 , RMSE=28	-----

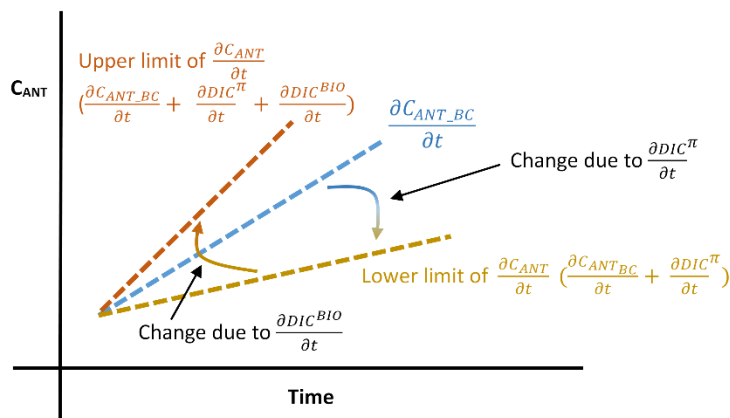


Table 5. Trends of anthropogenic carbon from estimates of the back-calculation method and of the terms DIC^{BIO} and DIC^{π} (see section 3.2 of the text). RMSE = root mean square error. Bottom: schematic of the estimation of the upper and lower limits of $\frac{\partial C_{\text{ANT}}}{\partial t}$ (see section 3.3).

Layers	Thickness (m)	C _{ANT} storage rates (mol m ⁻² yr ⁻¹)
STCW	230	[0.17 ± 0.06 - 0.22 ± 0.08]
AASW	280	[0.10 ± 0.04 - 0.24 ± 0.07]
AASW _{upw}	275	[0 - 0.11 ± 0.04]
SAMW	450	0.43 ± 0.14
AAIW	900	0.39 ± 0.14
SR03 section	---	0.30 ± 0.24

Table 6. Approximated rates of C_{ANT} storage based on the trends from Table 4.

Layer	$\partial C_{AN}/\partial t$ ($\mu\text{mol kg}^{-1} \text{yr}^{-1}$) 1995-2011	ΔC_{ANT} (Two-regression) ($\mu\text{mol kg}^{-1} \text{yr}^{-1}$) 1995-2011	ΔC_{ANT} (eMLR) ($\mu\text{mol kg}^{-1} \text{yr}^{-1}$) 1995-2011
STCW	[0.71 ± 0.08 - 0.93 ± 0.08]	0.72 ± 0.04, RMSE=5	1.21 ± 0.09, RMSE=3
AASW	[0.35 ± 0.14 - 0.85 ± 0.21]	0.61 ± 0.04, RMSE=6	0.67 ± 0.10, RMSE=10
AASW _{upw}	[0 - 0.41 ± 0.16]	0.20 ± 0.03, RMSE=3	0.30 ± 0.04, RMSE=3
SAMW	0.92 ± 0.09, RMSE=10	0.94 ± 0.05, RMSE=5	0.96 ± 0.09, RMSE=10
AAIW	0.42 ± 0.06, RMSE=10	0.28 ± 0.02, RMSE=4	0.43 ± 0.02, RMSE=7
UCDW	----	0.09 ± 0.01, RMSE=2	0.15 ± 0.09, RMSE=3
LCDW	----	0.08 ± 0.01, RMSE=2	0.28 ± 0.15, RMSE=3
AABW	** 0.07 ± 0.01, RMSE=2	0.09 ± 0.01, RMSE=1	0.18 ± 0.08, RMSE=2

Table 7. Comparison between $\frac{\partial C_{ANT}}{\partial t}$ from the present study and the values of ΔC_{ANT} from the two-regression and eMLR methods. RMSE= root mean square error. ** The value of $\frac{\partial C_{ANT}}{\partial t}$ in the AABW layer is considered negligible because it falls below the accuracy of the back-calculation method.

Carbon uptake and biogeochemical change in the Southern Ocean, south of Tasmania

Pardo, Paula C.¹, Tilbrook, Bronte^{1,2}, Langlais, Clothilde.², Trull, Tom W.^{1,2}, Rintoul, Steve R.^{1,2}


¹Antarctic Climate and Ecosystem Cooperative Research Centre, University of Tasmania, Hobart, Australia

²Climate Science Centre, CSIRO Oceans and Atmosphere, Hobart, Australia

Correspondence to: Paula C. Pardo (paula.condepardo@csiro.au)

A Supplementary material

A.1 Biogeochemical Model.

The 1/10° biogeochemical ocean simulation is based on the near-global Ocean Forecasting Australia Model configuration (OFAM3) (Oke et al., 2013) with 51 vertical layers (14 layers between the surface and 100 m depth and partial cells to better represent bottom topography), a resolution of 4.7km at 65°S, 7.8km at 45°S and a constant meridional resolution of 11 km. This configuration represents the frontal structure and filament nature of the ACC and captures much of the mesoscale variability and the development of baroclinic eddies (Langlais et al., 2011, 2015). OFAM3 includes the World Ocean Model of Biogeochemistry and Trophic dynamics (WOMBAT) (Kidston et al., 2011; Oke et al., 2013) that is based on a nutrient, phytoplankton, zooplankton and detritus model, with the addition of an O₂ and CO₂ cycle. The ocean model is based on the version 4p1d of the Geophysical fluid Dynamics Laboratory Modular Ocean Model (Griffies, 2009). Horizontal mixing is provided by the biharmonic Smagorinsky viscosity scheme (Griffies and Hallberg 2000), and vertical mixing by the K-profile parameterization (KPP, Large et al. 1994). It has two tracers of DIC, one that sees an (pre-industrial) atmospheric value of 280 ppm (natural carbon tracer), and a second tracer that sees the observed rising atmospheric pCO₂ (total carbon tracer). The BGC parameters used with WOMBAT are based on Oschlies and Schartau (2005), with extra parameters for the carbon cycle w et al., 2017).

The 1/10° simulation spans from 1979 to 2014, forced by 3-hourly Japanese 55-year Reanalysis (JRA-55; Kobayashi et al., 2015), using bulk formula (Large and Yeager, 2004) for wind stress, turbulent sensible and latent fluxes, and evaporation. As the model is not coupled to a sea-ice model, the effects of sea-ice on heat and freshwater fluxes are accounted for by the use of the JRA-55 sea ice coverage field to mask the applied atmospheric fields. Below 2000m, a non-adaptive relaxation keeps the deep-ocean close to the observed climatology but allows the climate changes signals to penetrate to the deep ocean.

The model BGC fields are initialised with fields constructed from observations. Specifically, the World Ocean Atlas is used to initialise nutrients (phosphorus) and oxygen (Garcia et al 2006a; Garcia et al. 2006b). The Global Ocean Data Analysis Project (GLODAP) is used to initialise alkalinity and dissolved carbon (Sabine et al. 2004; Key et al. 2004). Phytoplankton is initialised with SeaWIFS observation (NASA, 2014) and zooplankton is initialised as a fraction of phytoplankton (0.05). As the inclusion of the BGC component is computationally expensive, the BGC fields are only integrated between 1992 and 2014. This duration spans the era of relevant satellite sea-colour observations.

A.2 OMP analysis.

The OMP method (Thompson and Edwards, 1981; Tomczak, 1981; Mackas et al., 1987; Tomczak and Large, 1989) considers the water samples as nodes of a grid in which the different properties (e.g., S, θ , O₂) are measured. The OMP assumes that the value of each property is the result of the linear

mixing of the water masses characterizing the region of study, which are called end members or source water types (SWT) and whose characteristics are known. Thus, the value of each node can be expressed as a linear combination of the SWTs:

$$P_i = \sum_j^{Nj} (SWT_j * P_j + R_i * \Delta O_2)$$

where P_i is the value of the property i in the node, P_j is the value of the correspondent properties of the j SWT. Since some of the measured variables are non-conservative (e.g., O_2), biogeochemical terms have to be included in the mixing equations ($R_i * \Delta O_2$) that are based on Redfield ratios and considered constant (R_i , Broecker, 1974; Anderson and Sarmiento 1994; Martiny et al., 2013). Here we use $R_N=9$ and $R_P = 125$, referenced to the oxygen consumption (ΔO_2) which were the optima after a sensibility analysis (Álvarez et al., 2014). ΔO_2 is considered a conservative variable (see sensitivity analysis in section 6.4). These stoichiometric ratios are in agreement with previous studies (Le Jehan and Treguer, 1983; Verlenkar et al., 1990; Lourey and Trull, 2001, see section 4.4.2).

The system of equations (resulting from considering all the properties measured in each sample plus a mass balance equation) is normalized and solved by a least square method with a positive definite constraint to obtain the fractions of each of the SWTs characterizing the water sample and satisfying the mass balance equation.

Before solving the system, each equation is weighted (the mass equation presents the highest weight to ensure its conservation) based on the accuracy of the property and/or the variability in the region of study (Table A1). Weights were also adjusted so that the ratios between the Standard Deviations of the Residuals and the analytical error (ϵ , Table A1) were almost the same for all the SWT properties (Table A1).

Here we consider 11 SWTs that characterize the water masses of the SR03 section, i.e., those that best enclose the main features of the T/S diagram and of other properties of the water masses of the section (Fig. A1). The conservative properties (θ and S) were defined based on bibliography available (Table A1):

- In order to take into account the subtropical waters two points were defined as upper limits in the T/S diagram (Fig. A1). These end members correspond to the main properties of both the Zeehan Current (ZC) and the EAC arriving to the north part of the section (Fig. 1). The end member SWT_{STW15} represents the extension of the ZC ($\sim 15^\circ\text{C}$, ~ 35) in winter to the region south of Tasmania described by Cresswell (2000). The reference for the characterization of the subtropical waters from the EAC, i.e., SWT_{STW16} , is the southern component of the Subtropical Lower Water, characterized by Sokolov and Rintoul (2000) as waters in the range $16-22^\circ\text{C}$ and $35.5-35.7$. These two end members are considered together for the study as $SWT_{STW} = SWT_{STW16} + SWT_{STW15}$.
- Two end members are used to represent the seasonal warming of the AASW as it extends from the Antarctic shelf to latitudes of the SAF. SWT_{AASW} is the AASW described by Mosby (1934) and defined by Pardo et al. (2012). SWT_{SASW} represents the warmest type of AASW

found in summer based on Chaigneau et al. (2004). In our study, the two endmembers are considered together as $SWT_{AAS} = SWT_{AASW} + SWT_{SASW}$, as is the case of subtropical waters.

- HSSW is produced in coastal polynyas, where ice-formation creates salty surface waters (Orsi et al., 2002). This water is also the precursor in the formation of bottom waters. The definition of the end member SWT_{HSSW} was obtained from the study of Lacarra et al. (2011) within the Adélie -George V Land coast (Fig. 1), one of the areas of formation of ALBW.
- SWT_{SAMW} represents the core of the SAMW that is ventilated south of Tasmania (Rintoul and Bullister, 1999). We defined this end member as a point inside the cluster defined by Herraiz-Borreguero and Rintoul (2010) (8.5-9°C, 34.58-34.68).
- The end member characterizing AAIW, SWT_{AAIW} , is the variety of AAIW found south of Tasmania and close to the SAF and is defined by T of 4-4.5°C and S of 34.35 after Rintoul and Bullister, (1999).
- SWT_{NADW} reflects the properties of the NADW in South Atlantic, when it arrives to the ACC and is defined by Pardo et al. (2012).
- The end member SWT_{CDW} refers to waters in the deep bottom layers of the ACC that result from the mix with NADW arriving to the ACC, AAIW from above and the upper layers of the AABW, which, in specific locations of the Antarctic continent contributes to the formation of bottom waters. The properties of this end member are taken from Pardo et al. (2012).
- The end member SWT_{PIDW} refers to waters in the deep layers of the ACC (known as Lower Circumpolar Deep water) that are fed by deep waters from the Pacific and Indian Oceans and are characterized by a silicate maximum, high nutrients and low oxygen (e.g., Callahan, 1972; Whitworth et al., 1998). The values from the SWT_{PIDW} were obtained from Talley et al. (2011).
- SWT_{AABW} is the end member representing the bottom waters in the southern end of the section, close to the Antarctic shelf that result from a mixing between recently formed ALBW and RSBW. The definition of this end member is based on the observations from Rintoul and Bullister (1999).

The values of the non-conservative variables of the SWTs were initially extrapolated from regression lines with salinity and temperature (Poole and Tomczak, 1999) and then subjected to an iterative process in OMP in order to obtain the types that best fit the cruise data.

The number of SWTs included in the mixing depends on the number of properties measured at the node. In order to have enough degrees of freedom to solve the system of equations, we use combinations of water masses that we call mixing groups (Table A2), to solve different regions of the section. Each mixing group is connected to the other by one or more SWTs in order to maintain the

continuity of the analysis (Fig. A1), and are defined by considering the vertical characteristics and/or dynamics of the water masses in the region of study.


The robustness of the OMP analysis is tested through a perturbation analysis of uncertainties (Lawson and Hanson, 1974). The properties of both each SWT and each water sample are perturbed in order to check the sensitivity of the model to variations in the SWTs, due to environmental variability, and in the water samples, due to measurement errors (Leffaune and Tomczak, 2004). The uncertainties of the SWTs fractions (mean standard deviation of 100 perturbation runs) are shown together with the percentage of variability explained by the OMP analysis for each variable (Table A1). The model is reliable since it explains at least 98% of the variability of all the variables implicated (Table A1).

A.3 Parameterizations of TA^0 and CDIS.

The values of TA^0 and CDIS are defined for each SWT (Table A1) using the parameterizations and values from Pardo et al. (2011) and Pardo et al. (2014) (Table A3). Since mode and intermediate waters (SWT_{SAMW} and SWT_{AAIW} , Table A3) are formed and ventilated in areas influenced by subtropical waters and Antarctic waters, we combine the parameterizations for subtropical ([1]) and Antarctic ([2]) regions to obtain better values of both parameters (Table A3). The values of TA^0 and CDIS for the SWTs of mode and intermediate waters are estimated as $TA^0 = \frac{2}{3}(TA^0[1]) + \frac{1}{3}(TA^0[2])$ and $CDIS = \frac{2}{3}(CDIS[1]) + \frac{1}{3}(CDIS[2])$ (Table A2). The values obtain for TA^0 and CDIS for each SWT are then extended to the water column using the results from the OMP analysis:

$$TA^0 = \sum_{j=1}^{11} (SWT_j * TA_j^0); \quad CDIS = \sum_{j=1}^{11} (SWT_j * CDIS)$$

The appropriate combination of the parameterizations of TA^0 for the section is obtained by analysing the differences between TA and TA^0 at surface layers of the section, once TA^0 is determined by OMP analysis in order to avoid negative values. The values obtained for CDIS were very similar for all the SWTs except for SWT_{HSSW} , with an estimated CDIS value 4 times bigger than that some of the SWTs. Since the results from Landschutzer et al. (2015) indicate that the disequilibrium values do not change much between AASW and SAMW, we considered the value of CDIS obtained from the monthly mean values of atmospheric CO_2 from the NOAA network (1968-2015, Dlugokencky, et al., 2016) for latitudes $> 62^\circ S$, as the most appropriate for SWT_{HSSW} .

For the SWT_{NADW} , the value of TA^0 are obtained from the GLODAPv2 climatology (<http://cdiac.ornl.gov/oceans/GLODAPv2>; vset et al., 2016) in the area of the Indian Ocean and that of CDIS from Pardo et al. (2014). The SWTs for the rest of deep and bottom waters are formed by mixing of other water masses and the values of TA^0 and CDIS are obtained through an iterative process considering the composition of each SWT (Table A3) obtained from temperature and salinity. In the iterative process a default value is given to TA^0 and CDIS of SWT_{AABW} and iterations are run for the different deep-bottom water masses until the differences between the values of TA^0 and CDIS of two consecutive iterations are less than 0.005 for TA^0 and 0.05 for CDIS.

References.

Álvarez, M., Brea, S., Mercier, H. and Álvarez-Salgado, X.A.: Mineralization of biogenic materials in the water masses of the South Atlantic Ocean. I: assessment and results of an optimum multiparameter analysis, *Progress in Oceanography*, 123, 1-23, doi: 10.1016/j.pocean.2013.12.007, 2014.

Anderson, L.A. and Sarmiento, J.L.: Redfield ratios of remineralization determined by nutrient data analysis. *Global Biogeochemical Cycles* 8 (1), 65–80, doi: 10.1029/93GB03318, 1994.

Broecker, W.S.: “NO” a conservative water mass tracer. *Earth and Planetary Science Letters* 23, 8761–8776, 1974.

Callahan, J.E.: The structure and circulation of Deep Water in the Antarctic, *Deep-Sea Research*, 19, 563-575, 1972.

Chaigneau, A., Morrow, R.A. and Rintoul, S.R.: Seasonal and interannual evolution of the mixed layer in the Antarctic Zone south of Tasmania, *Deep-Sea Research I*, 51, 2047–2072, doi:10.1016/j.dsr.2004.06.013, 2004.

Cresswell, G.: Currents of the continental shelf and upper slope of Tasmania, In Banks, M.R. & Brown, M.J. (Eds): *Tasmania and the Southern Ocean*, Pap. Proc. R. Soc. Tasm., 133, 3, 21-30, 2000.

Dlugokencky, E.J., Lang, P.M., Mund, J.W., Crotwell, A.M., Crotwell, M.J. and Thoning, K.W.: Atmospheric Carbon Dioxide Dry Air Mole Fractions from the NOAA ESRL Carbon Cycle Cooperative Global Air Sampling Network, 1968-2015, Version: 2016-08-30, ftp://aftp.cmdl.noaa.gov/data/trace_gases/co2/flask/surface/, 2016.

Garcia, H.E., Locarnini, R.A., Boyer, T.P. and Antonov, J.I.: World ocean atlas 2005, volume 3: dissolved oxygen, apparent oxygen utilization, and oxygen saturation, In: Levitus, S. (Ed.), NOAA Atlas NESDIS 63. U.S. Government Printing Office, Washington, D.C., p. 342, 2006a.

Garcia, H.E., Locarnini, R.A., Boyer, T.P. and Antonov, J.I.: World ocean atlas 2005, volume 4: nutrients (phosphate, nitrate, silicate). In: Levitus, S. (Ed.), NOAA Atlas NESDIS 64. U.S. Government Printing Office, Washington, D.C., p. 396, 2006b.

Griffies, S.M., et al.: Coordinated Ocean-Ice Reference Experiments (COREs), *Ocean Modell.*, 26, 1–46, doi:10.1016/j.ocemod.2008.08.007, 2009.

Griffies, S.M. and Hallberg, R.W.: Biharmonic friction with a Smagorinsky viscosity for use in large-scale eddy permitting ocean models, *Mon. Weather Rev.* 128, 2935–2946, 2000.

Herraz-Borreguero, L. and Rintoul, S.R.: Subantarctic mode water variability influenced by mesoscale eddies south of Tasmania. *J. Geophys. Res.* 115, C04004, doi:10.1029/2008JC005146, 2010.

Key, R.M., et al.: A global ocean carbon climatology: Results from Global Data Analysis Project (GLODAP), *Global Biogeochem. Cycles*, 18, GB4031, doi:10.1029/2004GB002247, 2004.

Kidston, M., Matear, R. J. and Baird, M. E.: Parameter optimisation of a marine ecosystem model at two contrasting stations in the Sub-Antarctic Zone, *Deep-Sea Res.*, 58, 2301–2315, 2011.

Kobayashi, S., et al.: The JRA-55 Reanalysis: General specifications and basic characteristics. *J. Meteor. Soc. Japan*, 93, 5-48, doi:10.2151/jmsj.2015-001, 2015.


Lacarra, M., et al.: Summer hydrography on the shelf off Terre Adélie/George V Land based on the ALBION and CEAMARC observations during the IPY, *Polar Science*, 5, 2011, 88-103, doi:10.1016/j.polar.2011.04.008, 2011.


Landschützer, P., et al.: The reinvigoration of the Southern Ocean carbon sink, *Science*, 349, 1221–1224, doi:10.1126/science.aab2620, 2015.

Langlais, C., Rintoul, S. and Schiller, A.: Variability and mesoscale activity of the Southern Ocean fronts: Identification of a circumpolar coordinate system, doi:10.1016/j.ocemod.2011.04.010, *Ocean Modelling*, 39, 79–96, 2011.

Langlais, C.E., Rintoul, S.R. and Zika, J.D.: Sensitivity of Antarctic Circumpolar Current Transport and Eddy Activity to Wind Patterns in the Southern Ocean, *Journal of Physical Oceanography*, 45, 1051–1067, doi:10.1175/JPO-D-14-0053.1, 2015.

Large, W. G., McWilliams, J.C. and Doney, S.C.: Oceanic vertical mixing: a review and a model with a nonlocal boundary layer parameterization. *Rev. Geophys.*, 32, 363-403, 1994.

Large, W.G. and Yeager, S.G.: Diurnal to decadal global forcing for ocean and sea-ice models: the data sets and flux climatologies, TN-460+STR,  **AR technical note**, 111 pp, doi: 10.5065/D6KK98Q6, 2004.

 vset, S. K., et al.: A new global interior ocean mapped climatology: the 1°x1° GLODAP version 2, *Earth Syst. Sci. Data*, 8, 325–340, doi:10.5194/essd-8-325-2016, 2016.

Lawson, C.L. and Hanson, R.J.: *Solving Least Squares Problems*, Prentice-Hall, Englewood Cliffs, NJ., 1974.

 y, R. M. et al.: The carbon cycle in the Australian Community climate and Earth System Simulator (ACCESS-ESM1) Part 1: Model description and pre-industrial simulation, *Geosci. Model Dev.*, 10, 2567–2590, <https://doi.org/10.5194/gmd-10-2567-2017>, 2017.

Leffaune H. and Tomczak M.: Using OMP analysis to observe temporal variability in water mass distribution, *J. Mar. Syst.*, 48, 3–14, 2004.

Le Jehan, S. and Treguer, P.: Uptake and regeneration ASi/AN/AP ratios in the Indian Sector of the Southern Ocean. *Polar Biol.* 2: 127-136, 1983.

Lourey, K.J. and Trull, T.W.: Seasonal nutrient depletion and carbon export in the Subantarctic and Polar Frontal Zones of the Southern Ocean south of Australia, *J. Geophys. Res.*, 106, C12, 31,463–31,487, 2001.

Mackas, D.L., Denman, K.L. and Bennett, A.F.: Least squares multiple tracer analysis of water mass composition, *Journal of Geophysical Research*, 92, C3, 2907–2918, doi: 10.1029/JC092iC03p02907, 1987.

Martiny, A.C., et al.: Strong latitudinal patterns in the elemental ratios of marine plankton and organic matter, *Nature*, 6, 279-283, doi: 10.1038/NGEO1757, 2013.

Mosby, H.: *The waters of the Atlantic Antarctic Ocean, Scientific Results of the Norwegian Antarctic Expeditions 1927-1928*, 1, 11, 131 pp, 1934.

Oke, P.R., et al.: Evaluation of a near-global eddy-resolving ocean model, *Geosci. Model Dev.*, 6, 591–615, doi:10.5194/gmd-6-591-2013, 2013.

Orsi, A.H., Smethie Jr., W.M. and Bullister, J.L.: On the total input of Antarctic waters to the deep ocean: A preliminary estimate from chlorofluorocarbon measurements, *J. Geophys. Res.*, 107, C8, 3122, doi: 10.1029/2001JC000976, 2002.

Oschlies A. and Schartau, M.: Basin-scale performance of a locally optimized marine ecosystem model, *Journal of Marine Research*, 63, 2, 335-358, 2005.

Pardo, P.C., Vázquez-Rodríguez, M., Pérez, F.F. and Ríos, A.F.: CO₂ air-sea disequilibrium and preformed alkalinity in the Pacific and Indian Oceans calculated from subsurface layer data, *Journal of Marine Systems* 84, 67–77, doi:10.1016/j.jmarsys.2010.08.006, 2011.

Pardo, P.C., Perez, F.F., Velo, A. and Gilcoto, M.: Water masses distribution in the Southern Ocean: improvement of an extended OMP (eOMP) analysis. *Progress in Oceanography* 103, 92–105, doi: 10.1016/j.pocean.2012.06.00, 2012.

Pardo, P.C., Pérez, F.F., Khatiwala, S. and Ríos, A.F.: Anthropogenic CO₂ estimates in the Southern Ocean: Storage partitioning in the different water masses, *Progress in Oceanography*, 120, 230–242, doi:10.1016/j.pocean.2013.09.005, 2014.

Poole, R. and Tomczak, M.: Optimum multiparameter analysis of the water mass structure in the Atlantic Ocean thermocline, *Deep Sea Res., Part I*, 46, 1895– 1921, doi:10.1016/S0967-0637(99)00025-4, 1999.

Rintoul, S.R. and Bullister, J.L.: A late winter hydrographic section from Tasmania to Antarctica, *Deep –Sea Research I*, 46, 1417-1454, 1999.

Sabine, C.L., et al.: The Oceanic Sink for Anthropogenic CO₂, *Science*, 305, 5682, 367–371, 2004.

Sokolov, S. and Rintoul, S.R.: Circulation and water masses of the southwest Pacific: WOCE Section P11, Papua New Guinea to Tasmania, *Journal of Marine Research*, 58, 223–268, 2000.

Talley, L.D., Pickard, G.L., Emery, W.J. and Swift, J.H.: *Descriptive Physical Oceanography: An Introduction* (Sixth Edition), Elsevier, Boston, 560 pp, 2011.

Thompson, R.O. and Edwards, R.J., 1981. Mixing and water-mass formation in the Australian Subantarctic. *Journal of Physical Oceanography* 11, 1399–1406, 1981.

Tomczak, M.: A multi-parameter extension of temperature/salinity diagram techniques for the analysis of non-isopycnal mixing, *Progress in Oceanography*, 10, 147–171, 1981.

Tomczak, M. and Large, D.G.B.: Optimum Multiparameter Analysis of Mixing in the Thermocline of the Eastern Indian Ocean *Journal of Geophysical Research*, 94, C11, 16141-16149, 1989.

Verlencar, X.N., Somasunder, K. and Qasim, S.Z.: Regeneration of nutrients and biological productivity in Antarctic waters, *Marine Ecology Progress Series*, 61, 41-59, 1990.

Whitworth III, T., Orsi, A.H., Kim, S.-J. and Nowlin, W.D.: Water masses and mixing near the Antarctic Slope Front. *Antarctic Research Series*, 75, 1–27, 1998.

A Tables Supplementary material

	θ (°C)	S	SiO ₄ ($\mu\text{mol/kg}$)	NO ₃ ⁰ ($\mu\text{mol/kg}$)	PO ₄ ⁰ ($\mu\text{mol/kg}$)	O ₂ ⁰⁺ ($\mu\text{mol/kg}$)	TA ⁰ ($\mu\text{mol/kg}$)	DIC ⁿ _{SAT} ($\mu\text{mol/kg}$)	CDIS ($\mu\text{mol/kg}$)	CDIS ⁿ ($\mu\text{mol/kg}$)	Fractions uncertainties (%)
SWT _{STW16}	16 ± 0.06	35.1 ± 0.07	0.9 ± 0.2	1.2 ± 0.2	0.04 ± 0.3	243 ± 2	2290	1990	-19	1	0.04
SWT _{STW15}	15 ± 0.06	35.66 ± 0.07	0.6 ± 0.2	0 ± 0.2	0.12 ± 0.3	247 ± 2	2328	2026	-22	-2	0.04
SWT _{AASW}	-1.85 ± 0.006	33.8 ± 0.005	45 ± 2	30.7 ± 0.2	2.10 ± 0.3	360 ± 4	2289	2137	-23	-19	0.06
SWT _{SASW}	5 ± 0.008	33.8 ± 0.03	3 ± 0.2	23.3 ± 0.3	1.55 ± 0.5	310 ± 3	2264	2064	-13	-4	0.06
SWT _{HSSW}	-1.91 ± 0.08	34.71 ± 0.006	80 ± 1	28.3 ± 0.08	2.02 ± 0.03	300 ± 3	2351	2188	-21	0	0.08
SWT _{SAMW}	8.8 ± 0.02	34.63 ± 0.03	6 ± 0.6	13.2 ± 0.6	0.92 ± 0.8	280 ± 7	2290	2053	-10	2	0.03
SWT _{AIW}	4 ± 0.01	34.35 ± 0.02	34 ± 2	29.2 ± 0.4	1.97 ± 0.9	220 ± 8	2299	2099	-16	-6	0.04
SWT _{NADW}	3.28 ± 0.008	34.91 ± 0.003	28 ± 1	27.5 ± 0.3	1.19 ± 0.7	220 ± 4	2355	2152	-27	-10	0.08
SWT _{CDW}	0.65 ± 0.006	34.707 ± 0.003	115 ± 7	30.8 ± 0.1	2.12 ± 0.1	220 ± 3	2351	2168	-23	-2	0.03
SWT _{PDW}	1.44 ± 0.008	34.75 ± 0.005	125 ± 3	34.2 ± 0.01	3.4 ± 0.02	96 ± 2	2360	2168	-24	-4	0.04
SWT _{AABW}	-0.6 ± 0.006	34.66 ± 0.006	130 ± 5	30.7 ± 0.08	2.13 ± 0.03	259 ± 3	2355	2181	-22	-2	0.05
Weights	20	10	0.5	1	1	1					
SDR	0.004	0.003	6.0	0.50	0.04	2.0					
r ²	0.99	0.99	0.98	0.99	0.99	0.99					

Figure A1. Properties of the SWTs characterizing the water masses of the SR03 section with the correspondent accuracies (ϵ). All SWTs are defined with preformed values of the variables (ϵ). The values of preformed oxygen (O_2^0) are not in equilibrium for end members representing waters from the Antarctic shelf or old deep waters. The uncertainties in the fractions of the SWTs, the weights given to each variable in the OMP analysis, the Standard Deviation of the Residuals (SDR) and the square correlation coefficient (r^2) between the observed values and the OMP estimates are also listed.

Mixing Groups

STW15 + SAMW + SASW + STW16

SASW + SAMW + AAIW + AASW

SAMW + AAIW + NADW

AAIW + PIDW + NADW

AASW + AAIW + CDW

CDW + AABW + HSSW + AASW

Table A2. Mixing groups used in the OMP analysis. Note that only the subscripts of the names of the SWTs are written, i.e., STW15 instead of SWT_{STW15} .

SWTs	Parameterizations	Reference
SWT_{STW16}	$AT^{\circ} (\pm 6) = 2288.3 + 62.8*(S - 35) - 0.9*(\theta - 16) + 0.1*(PO - 300)$ $CDIS (\pm 5) = -47.9 + 2.31*\theta + 0.16*(PO - 300)$	Parameterizations for the South Subtropical region-Pacific Ocean (SSTIP, Pardo et al., 2011)
SWT_{STW15}	$AT^{\circ} (\pm 6) = 2288.3 + 62.8*(S - 35) - 1.6*(\theta - 16) + 0.1*(PO - 300)$ $CDIS (\pm 5) = 51.3 + 2.31*\theta + 0.16*(PO - 300)$	Parameterizations for the South Subtropical region-Indian Ocean (SSTIP, Pardo et al., 2011)
SWT_{HSSW}^*		Parameterizations for the Antarctic region (AAIP, Pardo et al., 2011) *(Dhugokencky, et al., 2016)
SWT_{AASW}	$AT^{\circ} (\pm 4) = 2296.7 + 94.7*(S - 35) + 0.3*(PO - 300)$ $CDIS (\pm 5) = -84.3 - 12.95*(S - 35) + 5.75*\theta + 0.17*(PO - 300)$	
SWT_{SASW}		
SWT_{SAMW}	$AT^{\circ}[1] (\pm 6) = 2288.3 + 62.8*(S - 35) - (0.9//1.6)*(\theta - 16) + 0.1*(PO - 300)$ $AT^{\circ}[2] (\pm 4) = 2296.7 + 94.7*(S - 35) + 0.3*(PO - 300)$ $CDIS[1] (\pm 5) = -47.9 + 2.31*\theta + 0.16*(PO - 300)$ $CDIS[2] (\pm 5) = -84.3 - 12.95*(S - 35) + 5.75*\theta + 0.17*(PO - 300)$	Parameterizations for the South Subtropical regions and for the Antarctic region (SSTIP, Pardo et al., 2011)
SWT_{AAIW}		
SWT_{NADW}	-----	GLODAPv2 // Pardo et al. (2014) **
SWT_{CDW}	$AT^{\circ} // CDIS = 0.69*(AT^{\circ} // CDIS)_{AABW} + 0.26*(AT^{\circ} // CDIS)_{NADW} +$ $0.05*(AT^{\circ} // CDIS)_{AAIW}$	-----
SWT_{PIDW}	$AT^{\circ} // CDIS = 0.71*(AT^{\circ} // CDIS)_{CDW} + 0.25*(AT^{\circ} // CDIS)_{NADW} +$ $0.04*(AT^{\circ} // CDIS)_{AAIW}$	-----
SWT_{AABW}	$AT^{\circ} // CDIS = 0.51*(AT^{\circ} // CDIS)_{CDW} + 0.44*(AT^{\circ} // CDIS)_{HSSW} +$ $0.05*(AT^{\circ} // CDIS)_{AASW}$	-----

Table A3. Parameterizations for estimating AT° and CDIS in each of the SWTs. $PO = R_p PO_4 + O_2$. For SWT_{HSSW}^* , CDIS is obtained from the NOAA database of latitudinal mean values of atmospheric CO_2 . For SWT_{NADW}^{**} , AT° is obtained from the climatology of GLODAPv2 and CDIS from Pardo et al. (2014).

B Figures Supplementary Material

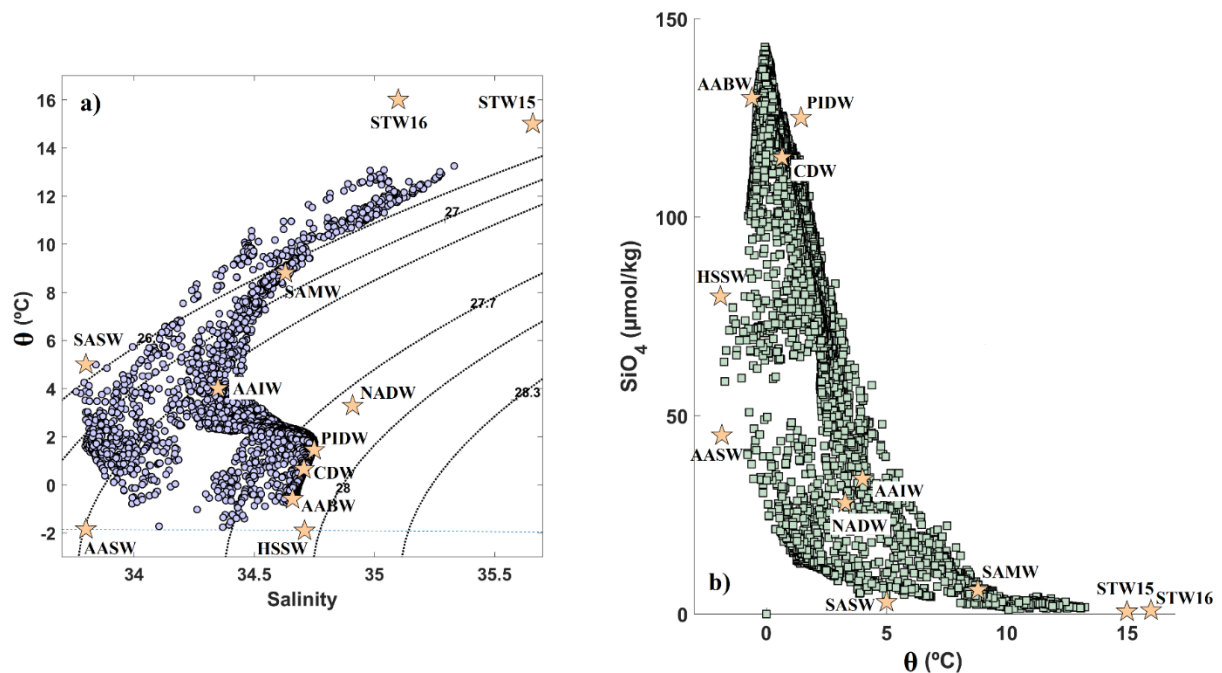
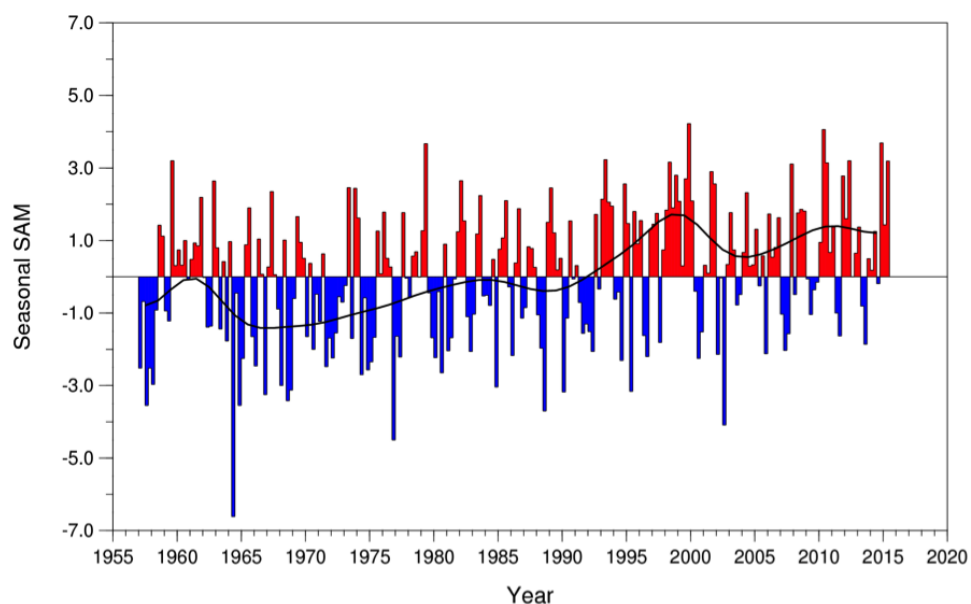


Fig. A1. (a) T/S diagram, with θ = potential temperature. Blue dots represent the data from all cruises for the period 1995-2011. Dotted lines indicate density (σ_θ , kg m⁻³). (b) SiO₄/T diagram, with θ = potential temperature. Green squares represent the data from all cruises for the period 1995-2011. Pentagrams represents the SWTs included in the OMP analysis (only subscripts are written, i.e., AASW instead of SWT_{AASW}).



A2. Seasonal values of the observation-based SAM index. The smooth black curve shows decadal variations. Figure obtained from Marshall, Gareth & National Center for Atmospheric Research Staff (Eds). "The Climate Data Guide: Marshall Southern Annular Mode (SAM) Index (Station-based)." Retrieved from <https://climatedataguide.ucar.edu/climate-data/marshall-southern-annular-mode-sam-index-station-based>.